

**Title:**

**Positive Biodiversity–Productivity Relationship Predominant in Global Forests**

**Short Title:**

**Global Biodiversity Effect on Forest Productivity**

**Authors:**

Jingjing Liang<sup>1\*</sup>, Thomas W. Crowther<sup>2</sup>, Nicolas Picard<sup>3</sup>, Susan Wiser<sup>4</sup>, Mo Zhou<sup>1</sup>, Giorgio Alberti<sup>5</sup>, Ernst-Detlef Schulze<sup>6</sup>, A. David McGuire<sup>7</sup>, Fabio Bozzato<sup>8</sup>, Hans Pretzsch<sup>9</sup>, Sergio de-Miguel<sup>10,11</sup>, Alain Paquette<sup>12</sup>, Bruno Hérault<sup>13</sup>, Michael Scherer-Lorenzen<sup>14</sup>, Christopher B. Barrett<sup>15</sup>, Henry B. Glick<sup>16</sup>, Geerten M. Hengeveld<sup>17,18</sup>, Gert-Jan Nabuurs<sup>17,19</sup>, Sebastian Pfautsch<sup>20</sup>, Helder Viana<sup>21,22</sup>, Alexander C. Vibrans<sup>23</sup>, Christian Ammer<sup>24</sup>, Peter Schall<sup>24</sup>, David Verbyla<sup>25</sup>, Nadja Tchebakova<sup>26</sup>, Markus Fischer<sup>27,28</sup>, James V. Watson<sup>1</sup>, Han Y.H. Chen<sup>29</sup>, Xiangdong Lei<sup>30</sup>, Mart-Jan Schelhaas<sup>17</sup>, Huicui Lu<sup>19</sup>, Damiano Gianelle<sup>31,32</sup>, Elena I. Parfenova<sup>26</sup>, Christian Salas<sup>33</sup>, Eungul Lee<sup>34</sup>, Boknam Lee<sup>35</sup>, Hyun Seok Kim<sup>35,36,37,38</sup>, Helge Bruelheide<sup>39,40</sup>, David A. Coomes<sup>41</sup>, Daniel Piotto<sup>42</sup>, Terry Sunderland<sup>43,44</sup>, Bernhard Schmid<sup>45</sup>, Sylvie Gourlet-Fleury<sup>46</sup>, Bonaventure Sonké<sup>47</sup>, Rebecca Tavani<sup>48</sup>, Jun Zhu<sup>49,50</sup>, Susanne Brandl<sup>9,51</sup>, Jordi Vayreda<sup>52,53</sup>, Fumiaki Kitahara<sup>54</sup>, Eric B. Searle<sup>29</sup>, Victor J. Neldner<sup>55</sup>, Michael R. Ngugi<sup>55</sup>, Christopher Baraloto<sup>56,57</sup>, Lorenzo Frizzera<sup>31</sup>, Radomir Bałazy<sup>58</sup>, Jacek Oleksyn<sup>59</sup>, Tomasz Zawila-Niedźwiecki<sup>60</sup>, Olivier Bouriaud<sup>61,62</sup>, Filippo Bussotti<sup>63</sup>, Leena Finér<sup>64</sup>, Bogdan Jaroszewicz<sup>65</sup>, Tommaso Jucker<sup>41</sup>, Fernando Valladares<sup>66</sup>, Andrzej M. Jagodzinski<sup>59,67</sup>, Pablo L. Peri<sup>68,69,70</sup>, Christelle Gonmadje<sup>47,71</sup>, William Marthy<sup>72</sup>, Timothy O'Brien<sup>72</sup>, Emanuel H. Martin<sup>73</sup>, Andrew R. Marshall<sup>74,75</sup>, Francesco Rovero<sup>76</sup>, Robert Bitariho<sup>77</sup>, Pascal A. Niklaus<sup>45</sup>, Patricia Alvarez-Loayza<sup>78</sup>, Nurdin Chamuya<sup>79</sup>, Renato Valencia<sup>80</sup>, Frédéric Mortier<sup>81</sup>, Verginia Wortel<sup>82</sup>, Nestor L. Engone-Obiang<sup>83</sup>, Leandro V. Ferreira<sup>84</sup>, David E. Odeke<sup>85</sup>, Rodolfo M. Vasquez<sup>86</sup>, Simon L. Lewis<sup>87,88</sup>, Peter B. Reich<sup>20,89</sup>

## **Affiliations:**

<sup>1</sup>School of Natural Resources, West Virginia University, Morgantown, WV 26505, USA.

<sup>2</sup>Netherlands Institute of Ecology, 6700 AB Wageningen, the Netherlands.

<sup>3</sup>Forestry Department, Food and Agriculture Organization of the United Nations, Rome, Italy.

<sup>4</sup>Landcare Research, Lincoln 7640, New Zealand.

<sup>5</sup>Department of Agri-Food, Animal and Environmental Sciences, University of Udine via delle Scienze 206, Udine 33100, Italy.

<sup>6</sup>Max-Planck Institut für Biogeochemie, Hans-Knoell-Strasse 10, 07745 Jena, Germany.

<sup>7</sup>U.S. Geological Survey, Alaska Cooperative Fish and Wildlife Research Unit, University of Alaska Fairbanks, Fairbanks, AK 99775 USA.

<sup>8</sup>Architecture & Environment Dept., Italcementi Group, 24100 Bergamo, Italy.

<sup>9</sup>Chair for Forest Growth and Yield Science, TUM School of Life Sciences Weihenstephan, Technical University of Munich, Hans-Carl-von-Carlowitz-Platz 2, 85354 Freising, Germany.

<sup>10</sup>Departament de Producció Vegetal i Ciència Forestal, Universitat de Lleida-Agrotecnio Center (UdL-Agrotecnio), Av. Rovira Roure, 191, E-25198 Lleida, Spain.

<sup>11</sup>Centre Tecnològic Forestal de Catalunya (CTFC), Ctra. De St. Llorenç de Morunys, km. 2. E-25280 Solsona, Spain.

<sup>12</sup>Centre d'étude de la forêt (CEF), Université du Québec à Montréal, Montréal, QC H3C 3P8, Canada.

<sup>13</sup>Cirad, UMR EcoFoG (AgroParisTech, CNRS, INRA, Université des Antilles, Université de la Guyane), Kourou, French Guiana.

<sup>14</sup>University of Freiburg, Faculty of Biology, Geobotany, D-79104 Freiburg, Germany.

<sup>15</sup>CH Dyson School of Applied Economics and Management, Cornell University, Ithaca, NY 14853 USA.

<sup>16</sup>Yale School of Forestry and Environmental Studies, New Haven, CT 06511, USA.

<sup>17</sup>Team Vegetation, Forest & Landscape Ecology, Alterra – 6700 AA Wageningen UR, Netherlands.

<sup>18</sup>Forest and Nature Conservation Policy Group, Wageningen University, 6700 AA Wageningen UR, Netherlands.

<sup>19</sup>Forest Ecology and [Forest](#) Management Group, Wageningen University, 6700 AA Wageningen UR, Netherlands.

<sup>20</sup>Hawkesbury Institute for the Environment, Western Sydney University, Richmond NSW 2753, Australia.

<sup>21</sup>CI&DETS Research Centre / DEAS-ESAV, Polytechnic Institute of Viseu, Portugal.

<sup>22</sup>Centre for the Research and Technology of Agro-Environmental and Biological Sciences, CITAB, University of Trás-os-Montes and Alto Douro, UTAD, Quinta de Prados, 5000-801 Vila Real, Portugal.

<sup>23</sup>Departamento de Engenharia Florestal, Universidade Regional de Blumenau, Rua São Paulo, 3250, 89030-000 Blumenau-Santa Catarina, Brazil.

<sup>24</sup>Department of Silviculture and Forest Ecology of the Temperate Zones, Georg-August University Göttingen, Büsgenweg 1, D-37077 Göttingen, Germany.

<sup>25</sup>School of Natural Resources and Extension, University of Alaska Fairbanks, Fairbanks, AK 99709, USA.

<sup>26</sup>V.N. Sukachev Institute of Forests, Siberian Branch, Russian Academy of Sciences, Akademgorodok, 50/28, 660036 Krasnoyarsk, Russia.

- <sup>27</sup>Institute of Plant Sciences, Botanical Garden, and Oeschger Centre for Climate Change Research, University of Bern, 3013 Bern, Switzerland.
- <sup>28</sup>Senckenberg Gesellschaft für Naturforschung, Biodiversity and Climate Research Centre (BIK-F), 60325 Frankfurt, Germany.
- <sup>29</sup>Faculty of Natural Resources Management, Lakehead University, Thunder Bay, ON P7B 5E1 Canada.
- <sup>30</sup>Research Institute of Forest Resource Information Techniques, Chinese Academy of Forestry, Beijing 100091, China.
- <sup>31</sup>Sustainable Agro-Ecosystems and Bioresources Department, Research and Innovation Centre - Fondazione Edmund Mach, Via E. Mach 1, 38010 - S. Michele all'Adige (TN), Italy.
- <sup>32</sup>Foxlab Joint CNR-FEM Initiative, Via E. Mach 1, 38010 - S. Michele all'Adige; Adige (TN), Italy.
- <sup>33</sup>Departamento de Ciencias Forestales, Universidad de La Frontera, Temuco, Chile.
- <sup>34</sup>Department of Geology and Geography, West Virginia University, Morgantown, WV 26505, USA.
- <sup>35</sup>Research Institute of Agriculture and Life Sciences, Seoul National University, Seoul, Republic of Korea.
- <sup>36</sup>Department of Forest Sciences, Seoul National University, Seoul 151-921, Republic of Korea.
- <sup>37</sup>Interdisciplinary Program in Agricultural and Forest Meteorology, Seoul National University, Seoul 151-744, Republic of Korea.
- <sup>38</sup>National Center for AgroMeteorology, Seoul National University, Seoul 151-744, Republic of Korea.
- <sup>39</sup>Institute of Biology / Geobotany and Botanical Garden, Martin Luther University Halle-Wittenberg, Am Kirchtor 1, 06108 Halle (Saale), Germany.
- <sup>40</sup>German Centre for Integrative Biodiversity Research (iDiv) Halle-Jena-Leipzig, Deutscher Platz 5e, 04103 Leipzig, Germany.
- <sup>41</sup>Forest Ecology and Conservation, Department of Plant Sciences, University of Cambridge, Cambridge CB2 3EA, UK.
- <sup>42</sup>Universidade Federal do Sul da Bahia, Ferradas, Itabuna 45613-204, Brazil.
- <sup>43</sup>Sustainable Landscapes and Food Systems, Centre for International Forestry Research, Bogor, Indonesia.
- <sup>44</sup>School of Marine and Environmental Studies, James Cook University, Australia.
- <sup>45</sup>Institute of Evolutionary Biology and Environmental Studies, University of Zurich, CH-8057 Zurich, Switzerland.
- <sup>46</sup>Département Environnements et Sociétés du CIRAD, 34398 Montpellier Cedex 5, France.
- <sup>47</sup>~~Plant Systematic and Ecology Laboratory, Department of Biology, Higher Teachers' Training College, Faculty of Sciences,~~ Department of Plant Ecology Laboratory, Department of Biology, Higher Teachers' Training College, Faculty of Sciences, University of Yaounde I, P.O. BOX 047812, Yaounde, Cameroon.
- <sup>48</sup>Forestry Department, Food and Agriculture Organization of the United Nations, Rome 00153, Italy.
- <sup>49</sup>Department of Statistics, University of Wisconsin-Madison, Madison, WI 53706 USA.
- <sup>50</sup>Department of Entomology, University of Wisconsin-Madison, Madison, WI 53706 USA.
- <sup>51</sup>Bavarian State Institute of Forestry, Hans-Carl-von-Carlowitz-Platz 1, Freising 85354, Germany.
- <sup>52</sup>Center for Ecological Research and Forestry Applications (CREAF), Cerdanyola del Vallès 08193, Spain.

- <sup>53</sup>Univ Autònoma Barcelona, Cerdanyola del Vallés 08193, Spain.
- <sup>54</sup>Shikoku Research Center, Forestry and Forest Products Research Institute, Kochi 780-8077, Japan.
- <sup>55</sup>Ecological Sciences Unit at Queensland Herbarium, Department of Science, Information Technology and Innovation, Queensland government, Toowong, Qld, 4066, Australia.
- <sup>56</sup>International Center for Tropical Botany, Department of Biological Sciences, Florida International University, Miami, FL 33199, USA.
- <sup>57</sup>INRA, UMR EcoFoG, Kourou, French Guiana.
- <sup>58</sup>Forest Research Institute, Sekocin Stary Braci Lesnej 3 Street, 05-090 Raszyn, Poland.
- <sup>59</sup>Institute of Dendrology, Polish Academy of Sciences, Parkowa 5, PL-62-035 Kornik, Poland.
- <sup>60</sup>Warsaw University of Life Sciences (SGGW), Faculty of Forestry, ul. Nowoursynowska 159, 02-776 Warszawa, Poland.
- <sup>61</sup>Forestry Faculty, University Stefan Cel Mare of Suceava, 13 Strada Universitații, 720229 Suceava, Romania.
- <sup>62</sup>Institutul Național de Cercetare-Dezvoltare în Silvicultură, 128 Bd Eroilor, 077190 Voluntari, Romania.
- <sup>63</sup>Department of Agri-Food Production and Environmental Science, University of Florence, P.le Cascine 28, 51044 Florence, Italy.
- <sup>64</sup>Natural Resources Institute Finland, 80101 Joensuu, Finland.
- <sup>65</sup>Białowieża Geobotanical Station, Faculty of Biology, University of Warsaw, Sportowa 19, 17-230 Białowieża, Poland.
- <sup>66</sup>Museo Nacional de Ciencias Naturales, CSIC Serrano 115 dpdo, E-28006 Madrid, Spain.
- <sup>67</sup>Poznan University of Life Sciences, Department of Game Management and Forest Protection, Wojska Polskiego 71c, PL-60-625 Poznan, Poland.
- <sup>68</sup>Consejo Nacional de Investigaciones Científicas y Técnicas (CONICET), Rivadavia 1917 (1033) Ciudad de Buenos Aires, Buenos Aires, Argentina.
- <sup>69</sup>INTA EEA Santa Cruz, Mahatma Gandhi 1322 (9400) Río Gallegos, Santa Cruz, Argentina.
- <sup>70</sup>Universidad Nacional de la Patagonia Austral (UNPA), Lisandro de la Torre 1070 (9400) Río Gallegos, Santa Cruz, Argentina.
- <sup>71</sup>National Herbarium, P.O. BOX 1601, Yaoundé, Cameroon.
- <sup>72</sup>Wildlife Conservation Society, Bronx NY 10460, USA.
- <sup>73</sup>College of African Wildlife Management, Department of Wildlife Management, P.O. Box 3031, Moshi, Tanzania.
- <sup>74</sup>Environment Department, University of York, Heslington, York, YO10 5NG, UK.
- <sup>75</sup>Flamingo Land Ltd., Malton, North Yorkshire, YO10 6UX.
- <sup>76</sup>Tropical Biodiversity Section, MUSE-Museo delle Scienze, Trento, Italy.
- <sup>77</sup>Institute of Tropical Forest Conservation, Kabale, Uganda.
- <sup>78</sup>~~Department of Evolutionary Biology and Environmental Studies, University of Zurich, Zurich, Switzerland.~~
- <sup>79</sup>~~Institute of Agricultural Sciences, ETH Zurich, Switzerland.~~
- <sup>78</sup>Center for Tropical Conservation, Durham, NC 27705, USA.
- <sup>79</sup>Ministry of Natural resources and Tourism, Forestry and Beekeeping Division, Dar es Salaam, Tanzania.
- <sup>80</sup>Escuela de Ciencias Biológicas, Pontificia Universidad Católica del Ecuador, Aptdo. 1701-2184, Quito, Ecuador.
- <sup>81</sup>CIRAD, UPR Bsef, Montpellier, 34398, France.

<sup>82</sup>Forest Management Department, CELOS, Paramaribo, Suriname

<sup>83</sup>Institut de Recherche Ecologie Tropicale (IRET/CENAREST), B.P. 13354, Libreville, Gabon

<sup>84</sup>Museu Paraense Emilio Goeldi, Coordenacao de Botanica, Belem, PA, Brasil.

<sup>85</sup>National Forest Authority, Kampala, Uganda.

<sup>86</sup>Prog. Bolognesi Mz-E-6, Oxapampa Pasco, Peru.

<sup>87</sup>Department of Geography, University College London, United Kingdom.

<sup>88</sup>School of Geography, University of Leeds, United Kingdom.

<sup>89</sup>Department of Forest Resources, University of Minnesota, St. Paul, MN 55108, USA.

\*Correspondence to: [albeca.liang@gmail.com](mailto:albeca.liang@gmail.com).

**Abstract:**

The biodiversity–productivity relationship (BPR) is foundational to our understanding of the global extinction crisis and its impacts on ecosystem functioning. Understanding BPR is critical for the accurate valuation and effective conservation of biodiversity. Using ground-sourced data from 777,126 permanent plots, spanning 44 countries and most terrestrial biomes, we reveal a globally consistent *positive concave-down* BPR, whereby a continued biodiversity loss would result in an accelerating decline in forest productivity worldwide. The value of biodiversity *in maintaining forest productivity*—US\$396–579 billion per year according to our estimation—is by itself over five times greater than the total cost of effective global conservation. This highlights the need for a worldwide re-assessment of biodiversity values, forest management strategies, and conservation priorities.

**One Sentence Summary:**

Global forest inventory records suggest that biodiversity loss would result in an accelerating decline in forest productivity worldwide.

The biodiversity–productivity relationship (BPR) has been a major ecological research focus over recent decades. The need to understand this relationship is becoming increasingly urgent in light of the global extinction crisis, as species loss affects the functioning and services of natural ecosystems (1, 2). In response to an emerging body of evidence which suggests that the functioning of natural ecosystems may be significantly impaired by reductions in species richness (3-10), global environmental authorities, including the Intergovernmental Platform on Biodiversity and Ecosystem Services (UN-IPBES) and United Nations Environment Programme (UNEP), have made substantial efforts to strengthen the preservation and sustainable use of biodiversity (2, 11). Successful international collaboration, however, requires a systematic assessment of the value of biodiversity (11). Quantification of the global BPR is thus urgently needed to facilitate the accurate valuation of biodiversity (12), the forecast of future changes in ecosystem services worldwide (11), and the integration of biological conservation into international socio-economic development strategies (13).

The evidence of a positive BPR stems primarily from studies of herbaceous plant communities (14). In contrast, the forest BPR has only been explored at regional scales (see 3, 4, 7, 15, and references therein) and limited tree-based experiments (see 16, 17, and references therein), and it remains unclear whether this relationship holds across forest types. Forests are the most important global repositories of terrestrial biodiversity (18), but deforestation, climate change, and other factors are threatening a considerable proportion (approximately 50%) of tree species worldwide (19-21). The consequences of this diversity loss pose a critical uncertainty for ongoing international forest management and conservation efforts. In contrast, forest management that converts monocultures to mixed-species stands has often seen a considerably substantial positive effect on productivity with many other benefits (e.g. 22, 23, 24).

Although forest plantations are predicted to meet 50–75% of the demand for lumber by 2050 (25), nearly all are still planted as monocultures, highlighting the potential of forest management in strengthening the conservation and sustainable use of biodiversity worldwide.

Here, we compiled *in situ* remeasurement data ~~(i.e. data, most of which were~~ taken at two consecutive inventories from the same localities~~)~~, from 777,126 permanent sample plots (hereafter, global forest biodiversity or GFB plots) across 44 countries/territories and 13 ecoregions to explore the forest BPR at a global scale (Fig.1). GFB plots encompass forests of various origins (from naturally regenerated to planted) and successional stages (from stand initiation to old-growth). A total of over thirty million trees across 8,737 species were tallied and measured on two or more consecutive inventories from the GFB plots. Sampling intensity was greater in developed countries, where nationwide forest inventories have been fully or partially funded by governments. In most other countries, national forest inventories were lacking and most ground-sourced data were collected by individuals and organizations (Data Table S1).

<Fig.1>

Based on ground-sourced GFB data, we quantified BPR at the global scale using a data-driven ensemble learning approach (see §Geospatial random forest in Materials and Methods). Our quantification of BPR involved characterizing the shape and strength of the dependency function, through the elasticity of substitution ( $\theta$ ), which represents the degree to which species can substitute for each other in contributing to forest productivity.  $\theta$  measures the marginal productivity – the change in productivity resulting from one unit decline of species richness, and reflects the strength of the effect of tree diversity on forest productivity, after accounting for climatic, soil, and plot specific covariates. A higher  $\theta$  corresponds to a greater decline in productivity due to one unit loss in biodiversity. The niche–efficiency (N–E) model (3) and

several preceding studies (26-29) provide a framework for interpreting the elasticity of substitution and approximating BPR with a power function model:

$$P = \alpha \cdot f(\mathbf{X}) \cdot S^\theta, \quad (1)$$

where  $P$  and  $S$  signify primary site productivity (~~derived from two consecutive inventories~~) and tree species richness (observed on a ~~400900~~-m<sup>2</sup> area basis on average, see Materials and Methods), respectively,  $f(\mathbf{X})$  a function of a vector of control variables  $\mathbf{X}$  (selected from stand basal area and 14 climatic, soil, and topographic covariates, ~~see Materials and Methods~~), and  $\alpha$  a constant. This model is capable of representing a variety of potential patterns of BPR.  $0 < \theta < 1$  represents a *positive and concave down* pattern (a degressively increasing curve) consistent with the N-E model and preceding studies (3, 26-29), whereas other  $\theta$  values can represent alternative BPR patterns, including decreasing ( $\theta < 0$ ), linear ( $\theta = 1$ ), convex ( $\theta > 1$ ), or no effect ( $\theta = 0$ ) (e.g. 14, 30) (Fig.2). The model (Eq.1) was estimated using the geospatial random forest technique based on GFB data and covariates acquired from ground-measured and remote sensing data (Materials and Methods).

<Fig.2>

We found that a positive biodiversity-productivity relationship (BPR) predominated forests worldwide. Out of 10,000 randomly selected subsamples (each consisting of 500 GFB plots), 99.87% had a *positive concave-down relationship* ( $0 < \theta < 1$ ), whereas only 0.13% show negative trends, and none was equal to zero, or was greater than or equal to 1 (Fig.2). Overall, the global forest productivity increased ~~degressively with a declining rate~~ from 2.7 to 11.8 m<sup>3</sup>ha<sup>-1</sup>yr<sup>-1</sup> as tree species richness increased from the minimum to the maximum value, which corresponds to a  $\theta$  value of 0.26 (Fig.3A).

<Fig.3>

At the global-scale, we mapped the magnitude of BPR (as expressed by  $\theta$ ) using geospatial random forest and universal kriging. Plotting values of  $\theta$  onto a global map shows considerable geospatial variation across the world (Fig.3B). The highest ~~elasticity of substitution~~  $\theta$  (0.29–0.30) occurred in the boreal ~~and temperate~~ forests ~~in of~~ North America, Northeastern Europe, Central Siberia, and East Asia; and ~~Asia, Mediterranean forests, and sporadic~~ tropical and subtropical forests ~~in of~~ South-central Africa, ~~Southeastern China~~ South-central Asia, and the ~~Oceania region~~ Malay Archipelago. In these areas of the highest elasticity of substitution ( $\theta$ ), the same percentage biodiversity loss would lead to greater percentage reduction in forest productivity (Fig.4A). In terms of absolute productivity, the same percentage biodiversity loss would lead to the greatest productivity decline in the Amazon, ~~Oceania~~, West Africa’s Gulf of Guinea, Southeastern Africa including Madagascar, Southern China, ~~and Northern~~ India Myanmar, Nepal, and the Malay Archipelago (Fig.4B). Due to a relatively narrow range of the elasticity of substitution ( $\theta$ ) estimated from the global-level analysis (0.2–0.3), the regions of the greatest productivity decline under the same percentage biodiversity loss largely matched the regions of the greatest productivity (Fig.S1). Globally, a 10 percent decrease ~~of in~~ tree species richness (from 100% to 90%) percent would cause a 2–3 percent decline in productivity, and with a 99 percent decrease of tree species richness (see §Economic analysis), this decline would escalate to 62–78 percent (Fig.4A).

<Fig.4>

## Discussion

Our global analysis provides strong and consistent evidence that productivity of forests worldwide would decrease at an accelerating rate with the loss of biodiversity. The positive concave-down pattern we discovered across forest ecosystems worldwide corresponds well with

recent theoretical advances in BPR (3, 27-29), as well as with experimental (e.g. 26) and observational (e.g. 14) studies on other forest and non-forest ecosystems. It is especially noteworthy that the elasticity of substitution (31) estimated in this study (ranged between 0.2 and 0.3) largely overlaps the range of values of the same exponent term (0.1–0.5) from previous theoretical and experimental studies (see 10, and references therein). Furthermore, our findings are consistent with the global estimates of the biodiversity-dependent ecosystem service debt under ~~distinct~~ assumptions distinct from previous theoretical and experimental results (10), and with recent reports of the diminishing marginal benefits of adding a species as species richness increases, based on long-term forest experiments ~~that dated~~dating back to 1870 (see 15, 32, and references therein).

Our analysis relied on stands ranging from unmanaged to extensively managed forests, i.e. managed forests with low operating and investment costs per unit area. It still remains a question if the positive concave-down BPR may be applicable to intensively managed forests (see §Natural vs. Managed Forests in Materials and Methods). Nevertheless, as intensively managed forests only account for a minor (<7%) portion of global forests (18), our estimated BPR would be minimally affected by such manipulations and thus should reflect the inherent processes governing the vast majority of global forest ecosystems.

We focused on the effect of biodiversity on ecosystem productivity. Recent studies on the opposite causal direction (i.e. productivity-biodiversity relationship, cf. 14, 33, 34) suggest that there may be a potential two-way causality between biodiversity and productivity. It is admittedly difficult to use correlative data to detect and attribute causal effects. Fortunately, substantial progress has been made to tease the BPR causal relationship from other potentially confounding environmental variables (14, 35, 36), and this study made considerable efforts to

account for these otherwise potentially confounding environmental covariates in assessing likely causal effects of biodiversity on productivity. Another feature that contributes to the interpretation that the effects in this study were causal was the fact that  $S$  represents tree species richness of the first inventory, whereas  $P$  is the average annual productivity between the two inventories. This temporal order reflects the BPR causality which requires the cause  $S$  to precede or coincide with the effect  $P$  in time (27).

Because taxonomic diversity indirectly incorporates functional, phylogenetic and genomic diversity, our results that focus on tree species richness are likely applicable to these other elements of biodiversity, all of which have been found to influence plant productivity (1). Such a straightforward analysis also makes it easier to understand the taxonomic contribution to forest ecosystem productivity and functioning, and the importance of preserving species diversity to biological conservation and forest management.

Our findings highlight the necessity to re-assess biodiversity valuation and re-evaluate forest management strategies and conservation priorities in forests worldwide. In terms of global carbon cycle and the global climate change, the value of biodiversity can be substantial as biodiversity maintains forest productivity and carbon stocks. Based on our global-scale analyses (Fig.4), the estimated size of forest carbon sink, and currently threatened number of tree species, a median level loss of threatened tree species (i.e. a 25% decrease of species richness from the current level) across the world in forest ecosystems worldwide (1, 21) could substantially reduce forest productivity and annual forest carbon absorption by 7.2 percent, adding an extra 0.14 petagrams per year (PgC yr<sup>-1</sup>) to current rate, which would in turn compromise the global carbon emissions forest land sink (37).

We further estimate that the economic value of biodiversity *in maintaining forest productivity* is

\$396–579 billion per year ( $\$3.96\text{--}5.79 \times 10^{11} \text{ yr}^{-1}$  in 2015 US\$, see §Economics Analysis in Materials and Methods). This value, representing only a small percentage of the *total* value of biodiversity (38, 39), is by itself over five times greater than the total cost of effective global conservation (\$76.1 billion per year (40)), thus ~~suggesting~~ underlining the need for a re-evaluation of forest management and conservation strategies.

Amid the struggle to combat biodiversity loss, the relationship between biological conservation and poverty is gaining increasing global attention (13, 41), especially in rural areas where livelihoods depend most directly on ecosystem products. Given the substantial geographic overlaps between severe, multifaceted poverty and key areas of global biodiversity (42), the loss of species in these areas has the potential to exacerbate local poverty ~~situations~~ situations by diminishing forest productivity and related ecosystem services (41). For example, in tropical and subtropical regions, many areas of high elasticity of substitution (31) overlapped with biodiversity hotspots (43), including Eastern Himalaya and Nepal, Mountains of Southwest China, Eastern Afromontane, Madrean pine-oak woodlands, Tropical Andes, and Cerrado. For these areas, only a few species of commercial value are targeted by logging, hence the risk of losing species through deforestation would far exceed the risk through harvesting (44). Deforestation and other anthropogenic drivers of biodiversity loss in these biodiversity hotspots may have high impacts on the productivity of forest ecosystems, exacerbating local poverty issues. Furthermore, the greater uncertainty in our results for the developing countries (Fig.5) reflects the well documented geographic bias in forest sampling including repeated measurements; and reiterates the need for strong commitments ~~are needed~~ towards improving sampling in the poorest regions of the world.

<Fig.5>

Our ~~study demonstrates findings, which reflect~~ the combined strength of large-scale integration and synthesis of ecological data and modern machine learning methods ~~in advancing understanding and quantification of a long-standing ecological issue. We have accounted for physiographic, climatic, and soil attributes in estimating the BPR to ensure that our estimates were not an artifact of potential confounding factors. These results,~~ increase our understanding of the consequences of global biodiversity loss, and the potential benefits of integrating and promoting biological conservation in forest resource management and forestry practices, a common goal already shared by intergovernmental organizations such as the Montréal and Helsinki Process Working Groups. These findings should facilitate efforts to accurately forecast future changes in ecosystem services worldwide—a primary goal of ~~UN-IPBES (11). Ultimately, our findings, and~~ provide baseline information necessary to establish international conservation objectives, including the UNCBD Aichi targets, the UNFCCC REDD+ goal, and the UNCCD land degradation neutrality goal~~;~~. The success of ~~which rely~~these goals relies on the understanding of the intrinsic link between biodiversity and forest productivity.

## Materials and Methods

### *Data collection and standardization*

Our current study used ground-sourced forest measurement data from 45 forest inventories collected from 44 countries and territories (Fig.1, Data Table S1). The measurements were collected in the field from predesignated sample area units, i.e. ~~GFB plots. For the calculation of primary site productivity,~~ Global Forest Biodiversity permanent sample plots (hereafter, GFB plots~~)). For the calculation of primary site productivity, GFB plots~~ can be categorized into two tiers. Plots designated as ‘Tier 1’ have been measured at two or more points in time with a

minimum time interval between measurements of two years or more (global mean time interval is 9 years, see Table 1). ‘Tier 2’ plots were only measured once and primary site productivity can be estimated from known stand age or dendrochronological records. Overall, our study was based on 777,126 GFB plots, of which 597,179 (77%) were Tier 1, and 179,798 (23%) were Tier 2. GFB plots primarily measured natural forests ranging from unmanaged to extensively managed forests, i.e. managed forests with low operating and investment costs per unit area. Intensively managed forests with harvests exceeding 50 percent of the stocking volume were excluded from this study. GFB plots represent forests of various origins (from naturally regenerated to planted) and successional stages (from stand initiation to old-growth).

For each GFB plot, we derived three key attributes from measurements of individual trees— tree species richness ( $S$ ), stand basal area ( $G$ ), and primary site productivity ( $P$ ). Because for each of all the GFB plot samples,  $S$  and  $P$  were derived from the measurements of the same trees, the sampling issues commonly associated with biodiversity estimation (45) had little influence on the  $S$ – $P$  relationship (i.e. BPR) in this study.

Species richness,  $S$ , represents the number of different tree species alive at the time of inventory within the perimeter of a GFB plot with an average size of approximately ~~400900~~ 400900 m<sup>2</sup>. Ninety-five percent of all plots fall between 100 and 1,100 m<sup>2</sup> in size. To minimize the species-area effect (e.g. 46), we studied the BPR here using a geospatial random forest model in which observations from nearby GFB plots would be more influential than plots that are farther apart (see §Geospatial random forest). Because nearby plots are most likely from the same forest inventory data set, and there was no or little variation of plot area within each data set, the BPR derived from this model largely reflected patterns under the same plot area basis. ~~Furthermore, because plot size~~ To investigate the potential effects of plot size on our results, we plotted the

estimated elasticity of substitution ( $\theta$ ) against plot size, and found that the scatter plot was normally distributed with no discernable pattern (Fig.S2). In addition, the fact that the plot size indicator  $I_2$  had the second lowest (0.8%) importance score (47) among all the covariates (Fig.6), further supports that the influence of plot size ~~on our results~~ variation in this study was negligible.

Across all the GFB plots there were 8,737 species in 1,862 genera and 231 families, and  $S$  values ranged from 1 to 405 per plot. We verified all the species names against 60 taxonomic databases, including NCBI, GRIN Taxonomy for Plants, Tropicos - Missouri Botanical Garden, and the International Plant Names Index, using the ‘taxize’ package in R (48). Out of 8,737 species recorded in the GFB database, 7,425 had verified taxonomic information with a matching score (48) of 0.988 or higher, whereas 1,312 species names partially matched existing taxonomic databases with a matching score between 0.50 and 0.75, indicating that these species may have not been documented in the 60 taxonomic databases. To facilitate inter-biome comparison, we further developed relative species richness ( $\check{S}$ ), a continuous percentage score converted from species richness ( $S$ ) and the local maximal species richness ( $S^*$ ) using

$$\check{S} = \frac{S}{S^*}. \quad (2)$$

Stand basal area ( $G$ , in  $\text{m}^2\text{ha}^{-1}$ ) represents the total cross-sectional area of live trees per unit sample area.  $G$  was calculated from individual tree diameter-at-breast-height ( $dbh$ , in cm):

$$G = 0.000079 \cdot \sum_i dbh_i^2 \cdot \kappa_i, \quad (3)$$

where  $\kappa_i$  denotes the conversion factor ( $\text{ha}^{-1}$ ) of the  $i$ th tree, *viz.* the number of trees per ha represented by that individual.  $G$  is a key biotic factor of forest productivity as it represents stand density— often used as a surrogate for resource acquisition (through leaf area) and stand

competition (49). Accounting for basal area as a covariate mitigated the artifact of different minimum dbh across inventories, and the artifact of different plot sizes.

Primary site productivity ( $P$ , in  $\text{m}^3\text{ha}^{-1}\text{yr}^{-1}$ ) was measured as tree volume productivity in terms of periodic annual increment (PAI) calculated from the sum of individual tree stem volume ( $V$ , in  $\text{m}^3$ ):

$$P = \frac{\sum_{i,2} V_{i,2} \cdot \kappa_i - \sum_{i,1} V_{i,1} \cdot \kappa_i + M}{Y}, \quad (4)$$

where  $V_{i,1}$  and  $V_{i,2}$  (in  $\text{m}^3$ ) represent total stem volume of the  $i$ th tree at the time of the first inventory and the second inventory, respectively.  $M$  denotes total removal of trees (including mortality, harvest, and thinning) in stem volume (in  $\text{m}^3\text{ha}^{-1}$ ).  $Y$  represents the time interval (in years) between two consecutive inventories.  $P$  accounted for mortality, ingrowth (i.e. recruitment between two inventories), and volume growth. Stem volume values were predominantly calculated using region- and species-specific allometric equations based on dbh and other tree- and plot-level attributes (Table 1). For the regions lacking an allometric equation, we approximated stem volume at the stand level from basal area, total tree height, and stand form factors (50). In case of missing tree height values from [the](#) ground measurement, we acquired alternative measures from a global 1-km forest canopy height database (51). For Tier 2 plots that lacked remeasurement,  $P$  was measured in mean annual increment (MAI) based on total stand volume and stand age (49), or tree radial growth measured from increment cores. Since the traditional MAI metric does not account for mortality, we calculated  $P$  by adding to MAI the annual mortality based on regional-specific forest turnover rates (52). The small and insignificant correlation coefficient between  $P$  and the indicator of plot tier ( $I_1$ ), together with the negligible

variable importance of  $I_1$  (1.8%, Fig.6) indicate that PAI and MAI were generally consistent so that MAI could be a good proxy of PAI in our study. Although MAI and PAI have considerable uncertainty in any given stand, it is difficult to see how systematic bias across diversity gradients could occur on a scale sufficient to influence the results shown here. Additionally, although other measures of productivity (e.g. net ecosystem exchange processed to derive gross and net primary production; direct measures of aboveground net primary production including all components; and remotely sensed estimates of LAI and greenness coupled with models) all have their advantages and disadvantages, none would be feasible at a similar scale and resolution as in this study.

<Table 1>

To account for abiotic factors that may influence primary site productivity, we ~~selected~~compiled 14 geospatial covariates based on biological relevance and spatial resolution (Fig.6). These covariates, derived from satellite-based remote sensing and ground-based survey data, can be grouped into three categories: climatic, soil, and topographic (Table 1). We preprocessed all geospatial covariates using ArcMap 10.3 (53) and R 2.15.3 (54). All covariates were extracted to point locations of GFB plots, with a nominal resolution of ~~1 km<sup>2</sup>~~1 km<sup>2</sup>.

<Fig.6>

### ***Geospatial random forest***

We developed geospatial random forest— a data-driven ensemble learning approach— to characterize biodiversity–productivity relationship (BPR), and to map BPR in terms of elasticity of substitution (31) on all sample sites across the world. This approach was developed to overcome two major challenges that arose from the size and complexity of GFB data without

assuming any underlying BPR patterns or data distribution. Firstly, we need to account for broad-scale differences in vegetation types, but global classification and mapping of homogeneous vegetation types is lacking (55); and secondly, correlations and trends that naturally occur through space (56) can be significant and influential in forest ecosystems (57). Geostatistical models have been developed to address the spatial autocorrelation, but due to the size of the GFB data set far exceeds the computational constraints, of most geostatistical models cannot be applied to account for spatial autocorrelation.

Geospatial random forest integrated conventional random forest (47) and a geostatistical nonlinear mixed-effects model (58) to estimate BPR across the world based on GFB plot data and their spatial dependence. The underlying model had the following form:

$$\log P_{ij}(\mathbf{u}) = \theta_i \cdot \log \tilde{S}_{ij}(\mathbf{u}) + \boldsymbol{\alpha}_i \cdot \mathbf{X}_{ij}(\mathbf{u}) + e_{ij}(\mathbf{u}), \quad \mathbf{u} \in \mathcal{D} \subset \mathfrak{R}^2, \quad (5)$$

where  $\log P_{ij}(\mathbf{u})$  and  $\log \tilde{S}_{ij}(\mathbf{u})$  represent natural logarithm of productivity and relative species richness (calculated from actual species richness and the maximal species richness of the training set) of plot  $i$  in the  $j$ th training set at point locations  $\mathbf{u}$ , respectively. The model was derived from the niche–efficiency model, and  $\theta$  corresponds to the elasticity of substitution (31).  $\boldsymbol{\alpha}_i \cdot \mathbf{X}_{ij}(\mathbf{u}) = \alpha_{i0} + \alpha_{i1} \cdot x_{ij1} + \dots + \alpha_{in} \cdot x_{ijn}$  represents  $n$  covariates and their coefficients (Fig.6, Table 1).

To account for potential spatial autocorrelation, which can bias tests of significance due to the violation of independence assumption and is especially problematic in large-scale forest ecosystem studies (56, 57), we incorporated a spherical variogram model (59) into the residual term  $e_{ij}(\mathbf{u})$ . The underlying geostatistical assumption was that across the world the gradient in BPR is inherently spatial— a common geographical phenomenon in which neighboring points are more similar to each other than they are to points that are more distant (60). In our study, we

found strong evidence for this gradient (Fig.7), indicating that observations from nearby GFB plots would be more influential than plots that are farther away. The positive spherical semivariance curves estimated from a large number of bootstrapping iterations indicated that spatial dependence increased as plots became closer together.

<Fig.7>

The aforementioned geostatistical nonlinear mixed-effects model was integrated into random forest (47) by means of model selection and estimation. In the model selection process, random forest was employed to assess the contribution of each of the candidate variables to the dependent variable  $\log P_{ij}(\mathbf{u})$ , in terms of the amount of increase in prediction error as one variable is permuted while all the others are kept constant. We used the randomForest package (61) in R to obtain importance measures for all the covariates to guide our selection of the final variables in the geostatistical nonlinear mixed-effects model,  $\mathbf{X}_{ij}(\mathbf{u})$ . We selected stand basal area ( $G$ ), temperature seasonality ( $T_3$ ), annual precipitation ( $C_1$ ), precipitation of the warmest quarter ( $C_3$ ), potential evapotranspiration ( $PET$ ), indexed annual aridity ( $IAA$ ), and plot elevation ( $E$ ) as control variables since their importance measures were greater than the 9 percent threshold (Fig.6) preset ~~in order for~~ to ensure that the final variables ~~to~~ account for over 60 percent of the total variable importance measures.

For geospatial random forest analysis of BPR, we first selected control variables based on the variable importance measures derived from random forests (47). We then evaluated the values of elasticity of substitution (31), which are expected to be real numbers greater than 0 and less than 1, against the alternatives, *i.e.* negative BPR ( $H_{01}: \theta < 0$ ), no effect ( $H_{02}: \theta = 0$ ), linear ( $H_{03}: \theta = 1$ ), and convex positive BPR ( $H_{04}: \theta > 1$ ). We examined all the coefficients by their statistical

significance, and effect sizes, using Akaike information criterion (AIC), Bayesian information criterion (BIC), and the generalized coefficient of determination (62).

### ***Global analysis***

For the global-scale analysis, we calibrated the nonlinear mixed-effects model parameters ( $\theta$  and  $\alpha$ 's) using a subset of sample points consisting of training sets of 500 plots randomly selected (with replacement) from the GFB global dataset according to the bootstrap aggregating (bagging) algorithm. We calibrated a total of 10,000 models based on the bagging samples, using our own bootstrapping program and the nonlinear package nlme (58) of R, to ~~get~~calculate the means and standard errors of final model estimates (Table 2). This approach overcame computational limits by partitioning the GFB sample into smaller subsamples to enable the nonlinear estimation. The size of training sets was selected based on the convergence and effect size of the geospatial random forest models. In pilot simulations with increasing sizes of training sets (Fig.8), the value of elasticity of substitution (31) fluctuated at the start until the convergence point at 500 plots. Generalized  $R^2$  value declined as the size of training sets increased from 0 to 350 plots, and stabilized at around 0.35 as training set size increased further. Accordingly, we selected 500 as the size of the training sets for the final geospatial random forest analysis. Based on the estimated parameters of the global model (Table 2), we analyzed the effect of relative species richness on global forest productivity with a sensitivity analysis by keeping all the other variables constant at their sample means for each ecoregion.

<Fig.8>

<Table 2>

### ***Mapping BPR across global forest ecosystems***

For ~~the~~ mapping purposes, we first estimated the current extent of global forests in several steps. We aggregated the 'treecover2000' and 'loss' data (63) from 30m pixels to 30 arc-second pixels (~1km) ~~while taking a mean~~ by calculating the respective means. The result was ~1km pixels showing the percentage forest cover for the year 2000 and the percentage of this forest cover lost between 2000 and 2013, respectively. The aggregated forest cover loss was multiplied by the aggregated forest cover to produce a single raster ~~where~~ value for each ~1km pixel ~~had~~ representing a percentage forest lost between 2000 and 2013. This multiplication was necessary since the initial loss ~~was only~~ values were relative to initial forest cover. Similarly, we estimated the percentage forest cover gain by aggregating the forest 'gain' data (63) from 30m to 30 arc-seconds ~~while taking a mean~~ and calculating the respective means. Then, this gain layer was multiplied by 1 minus the aggregated forest cover ~~noted in~~ from the first step to produce a single ~~raster where~~ value for each ~1km pixel ~~had~~ that signifies percentage forest gain from 2000–2013. This multiplication ensured that the gain could only occur in ~~proportion to~~ areas that were not already forested. Finally, the percentage forest cover for 2013 was computed by taking the aggregated data from the first step (year 2000) and subtracting the computed loss and adding the computed gain.

We mapped productivity  $P$  and elasticity of substitution (31) across the estimated current extent of global forests, here defined as areas with 50 percent or more forest cover. Because GFB ground plots represent approximately 40 percent of the forested areas, we used universal kriging (cf. 59) to estimate  $P$  and  $\theta$  for the areas with no GFB sample coverage. The universal kriging models consisted of covariates specified in Fig.6(B) and a spherical variogram model with parameters (i.e. nugget, range, and sill) specified in Fig.7. We obtained the best linear unbiased estimators of  $P$  and  $\theta$  and their standard error across the current global forest extent with the

*gstat* package of R (64). By combining  $\theta$  estimated from geospatial random forest and universal kriging, we produced the spatially continuous maps of the elasticity of substitution (Fig.3B) and forest productivity (Fig.S1) at a global scale. The effect sizes of the best linear unbiased estimator of  $\theta$  (in terms of standard error and generalized  $R^2$ ) ~~were~~ are shown in Fig.5. We further estimated percentage and absolute decline in worldwide forest productivity under two ~~levels—low (10% loss), and high (99% loss)—scenarios~~ of loss in tree species richness ~~(Fig.4), that is, —~~ low (10% loss) and high (99% loss). These levels represent the productivity decline (in both percentage and absolute terms) if local species richness across the global forest extent would ~~descend~~ decrease to 90 and 1 percent of the current values, respectively. The percentage decline was calculated based on the general BPR model (Eq.1) and estimated worldwide spatially explicit values of the elasticity of substitution (Fig.3B). The absolute decline was the product of the worldwide estimates of primary forest productivity (Fig.S1) and the standardized percentage decline ~~in response to~~ at the two levels of biodiversity loss (Fig.4A).

### *Natural vs. Managed Forests*

Our analysis relies on stands ranging from unmanaged to extensively managed forests, i.e. managed forests with low operating and investment costs per unit area, and excludes intensively managed forests with harvests exceeding 50 percent of the stocking volume. Conditions of natural forests would not be comparable to intensively managed forests, ~~for~~ as timber production in the latter systems often focuses on single or limited number of highly productive tree species. Intensively managed forests, where saturated resources can weaken the effects of niche–efficiency (3), ~~may have higher productivity than natural diverse forests of the same climate and site conditions. For example, the average productivity of managed forests of Germany with one to five species can be as high as the unmanaged productivity with 100 species in the tropics~~ are

~~shown in some studies (65, 66). Furthermore, if the native German tree species would be replaced by a single highly productive species, such as *Pseudotsuga menziesii*, productivity is expected to increase to 23–50 m<sup>3</sup>ha<sup>-1</sup>y<sup>-1</sup>. Thus, the positive concave-down productivity–biodiversity curve may not hold with intensive management have higher productivity than natural diverse forests of the same climate and site conditions (Fig.S2S3). In contrast, some intensively managed forests, other studies (e.g. 6, 22-24) compared diverse stands to monocultures at the same level of management intensity, also show and found that the positive effects of species diversity on tree productivity and other ecosystem services, suggesting that is still applicable to intensively managed forests. As such, there is still an unresolved debate on the BPR of intensively managed forests.~~

### ***Economic Analysis***

Estimates of the economic value-added from forests employ a range of methods. One prominent recent global valuation of ecosystem services (67) valued global forest production (in terms of ‘raw materials’ provided by forests (Table S1 in 67)) in 2011 at US\$ 649 billion ( $6.49 \times 10^{11}$ , in constant 2007 dollars). Using an alternative method, the UN FAO (25) estimates gross value-added in the formal forestry sector at US\$606 billion ( $6.06 \times 10^{11}$ , in constant 2011 dollars). We used these two reasonably comparable values as bounds on our coarse estimate of the global economic value of forest productivity, converted to constant 2015 US\$ based on the US consumer price indices (68). As indicated by our global-scale analyses (Fig.4A), a 10 percent decrease of tree species richness distributed evenly across the world (from 100% to 90%) would cause a 2.1–3.1 percent decline in productivity which would equate to US\$13–23 billion per year (constant 2015 US\$). At extremes, a sharp 99 percent drop ~~of~~in species richness would lead to

62–78% reduction in forest productivity, equivalent to 396–579 billion US\$ per year (3.96–5.79×10<sup>11</sup>, constant 2015 US\$).

~~The aforementioned~~ Even though these estimates of the economic value-added from forest BPR ~~came from~~ employed two starkly different methods ~~but, they~~ were still reasonably close. We held forested area and other factors constant to estimate the value of productivity loss solely due to a decline in tree species richness, ~~and hence the figures.~~ As such, these estimates did not include the value of land converted from forest and losses due to associated fauna and flora decline, and forest habitat reduction. This estimate only reflects the value of biodiversity *in maintaining forest wood productivity*, and does not account for other values of biodiversity. The *total* global value of biodiversity could exceed this estimate by magnitudes (38, 39):.

## REFERENCES AND NOTES

1. S. Naeem, J. E. Duffy, E. Zavaleta, The Functions of Biological Diversity in an Age of Extinction. *Science* **336**,1401-1406 (2012).
2. Millennium Ecosystem Assessment, “Ecosystems and Human Well-being: Biodiversity Synthesis ” (World Resources Institute, Washington, DC, 2005)
3. J. Liang, M. Zhou, P. C. Tobin, A. D. McGuire, P. B. Reich, Biodiversity influences plant productivity through niche–efficiency. *PNAS* **112**,5738-5743 (2015).
4. M. Scherer-Lorenzen, in *Forests and Global Change*, D. Burslem, D. Coomes, W. Simonson, Eds. (Cambridge University Press, Cambridge, 2014), pp. 195-238.
5. B. J. Cardinale *et al.*, Biodiversity loss and its impact on humanity. *Nature* **486**,59-67 (2012).
6. Y. Zhang, H. Y. H. Chen, P. B. Reich, Forest productivity increases with evenness, species richness and trait variation: a global meta-analysis. *J. Ecol.* **100**,742-749 (2012).
7. A. Paquette, C. Messier, The effect of biodiversity on tree productivity: from temperate to boreal forests. *Global Ecol. Biogeogr.* **20**,170-180 (2011).
8. P. Ruiz - Benito *et al.*, Diversity increases carbon storage and tree productivity in Spanish forests. *Global Ecol. Biogeogr.* **23**,311-322 (2014).
9. F. van der Plas *et al.*, Biotic homogenization can decrease landscape-scale forest multifunctionality. *PNAS* **113**,3557-3562 (2016).
10. F. Isbell, D. Tilman, S. Polasky, M. Loreau, The biodiversity-dependent ecosystem service debt. *Ecol. Lett.* **18**,119-134 (2015).
11. S. Díaz *et al.*, The IPBES Conceptual Framework — connecting nature and people. *Current Opinion in Environmental Sustainability* **14**,1-16 (2015).
12. United Nations. (Nagoya, Japan, 2010), vol. COP 10 Decision X/2.
13. W. M. Adams *et al.*, Biodiversity Conservation and the Eradication of Poverty. *Science* **306**,1146-1149 (2004).
14. J. B. Grace *et al.*, Integrative modelling reveals mechanisms linking productivity and plant species richness. *Nature* **529**,390–393 (2016).
15. D. I. Forrester, H. Pretzsch, Tamm Review: On the strength of evidence when comparing ecosystem functions of mixtures with monocultures. *For. Ecol. Manage.* **356**,41-53 (2015).
16. C. M. Tobner *et al.*, Functional identity is the main driver of diversity effects in young tree communities. *Ecol. Lett.* **19**,638-647 (2016).
17. K. Verheyen *et al.*, Contributions of a global network of tree diversity experiments to sustainable forest plantations. *Ambio* **45**,29-41 (2016).
18. FAO, “Global Forest Resources Assessment 2015 - How are the world’s forests changing? ” (Food and Agriculture Organization of the United Nations, Rome, Italy, 2015)
19. H. Ter Steege *et al.*, Estimating the global conservation status of more than 15,000 Amazonian tree species. *Science advances* **1**,e1500936 (2015).
20. R. Fleming, N. Brown, J. Jenik, P. Kahumbu, J. Plesnik, in *UNEP Year Book 2011* United Nations Environment Program, Ed. (UNEP, Nairobi, Kenya, 2011), pp. 46-59.
21. IUCN, *IUCN Red List Categories and Criteria: Version 3.1*. Version 2011.1. (Gland, Switzerland and Cambridge, UK, ed. 2nd, 2012), vol. iv, pp. 32.

22. H. Pretzsch, G. Schütze, Transgressive overyielding in mixed compared with pure stands of Norway spruce and European beech in Central Europe: evidence on stand level and explanation on individual tree level. *Eur. J. For. Res.* **128**,183-204 (2009).
23. A. Bravo-Oviedo *et al.*, European Mixed Forests: definition and research perspectives. *Forest Systems* **23**,518-533 (2014).
24. K. B. Hulvey *et al.*, Benefits of tree mixes in carbon plantings. *Nature Climate Change* **3**,869-874 (2013).
25. FAO, “Contribution of the forestry sector to national economies, 1990-2011” (Food and Agriculture Organization of the United Nations Rome, 2014). Value-added has been adjusted for inflation and is expressed in USD at 2011 prices and exchange rates.
26. B. J. Cardinale *et al.*, The functional role of producer diversity in ecosystems. *Am. J. Bot.* **98**,572-592 (2011).
27. P. B. Reich *et al.*, Impacts of biodiversity loss escalate through time as redundancy fades. *Science* **336**,589-592 (2012).
28. M. Loreau, A. Hector, Partitioning selection and complementarity in biodiversity experiments. *Nature* **412**,72-76 (2001).
29. D. Tilman, C. L. Lehman, K. T. Thomson, Plant diversity and ecosystem productivity: Theoretical considerations. *PNAS* **94**,1857-1861 (1997).
30. H. Y. H. Chen, K. Klinka, Aboveground productivity of western hemlock and western redcedar mixed-species stands in southern coastal British Columbia. *For. Ecol. Manage.* **184**,55-64 (2003).
31. The elasticity of substitution ( $\theta$ ), which represents the degree to which species can substitute for each other in contributing to stand productivity, reflects the strength of the effect of biodiversity on ecosystem productivity, after accounting for climatic, soil, and other environmental and local covariates.
32. H. Pretzsch *et al.*, Growth and yield of mixed versus pure stands of Scots pine (*Pinus sylvestris* L.) and European beech (*Fagus sylvatica* L.) analysed along a productivity gradient through Europe. *Eur. J. For. Res.* **134**,927-947 (2015).
33. J. Liang, J. V. Watson, M. Zhou, X. Lei, Effects of productivity on biodiversity in forest ecosystems across the United States and China. *Conserv. Biol.* **30**,308-317 (2016).
34. L. H. Fraser *et al.*, Worldwide evidence of a unimodal relationship between productivity and plant species richness. *Science* **349**,302-305 (2015).
35. M. Loreau, Biodiversity and ecosystem functioning: a mechanistic model. *PNAS* **95**,5632-5636 (1998).
36. F. Isbell *et al.*, Nutrient enrichment, biodiversity loss, and consequent declines in ecosystem productivity. *PNAS* **110**,11911-11916 (2013).
37. C. Le Quéré *et al.*, Global carbon budget 2015. *Earth System Science Data* **7**,349-396 (2015).
38. A. Hector, R. Bagchi, Biodiversity and ecosystem multifunctionality. *Nature* **448**,188-190 (2007).
39. L. Gamfeldt *et al.*, Higher levels of multiple ecosystem services are found in forests with more tree species. *Nat Commun* **4**,1340 (2013).
40. D. P. McCarthy *et al.*, Financial Costs of Meeting Global Biodiversity Conservation Targets: Current Spending and Unmet Needs. *Science* **338**,946-949 (2012).
41. C. B. Barrett, A. J. Travis, P. Dasgupta, On biodiversity conservation and poverty traps. *PNAS* **108**,13907-13912 (2011).

42. B. Fisher, T. Christopher, Poverty and biodiversity: Measuring the overlap of human poverty and the biodiversity hotspots. *Ecol. Econ.* **62**,93-101 (2007).
43. N. Myers, R. A. Mittermeier, C. G. Mittermeier, G. A. B. da Fonseca, J. Kent, Biodiversity hotspots for conservation priorities. *Nature* **403**,853-858 (2000).
44. S. Gourlet-Fleury, J.-M. Guehl, O. Laroussinie, *Ecology and management of a neotropical rainforest: lessons drawn from Paracou, a long-term experimental research site in French Guiana.* (Elsevier Paris, France, 2004), pp. 326.
45. J. C. Tipper, Rarefaction and rarefaction—the use and abuse of a method in paleoecology. *Paleobiology* **5**,423-434 (1979).
46. M. L. Rosenzweig, *Species Diversity in Space and Time.* (Cambridge University Press, Cambridge, 1995), pp. 436.
47. L. Breiman, Random forests. *Machine learning* **45**,5-32 (2001).
48. S. Chamberlain, E. Szocs, Taxize - taxonomic search and retrieval in R. *F1000Research* **2**,191 (2013).
49. B. Husch, T. W. Beers, J. A. Kershaw Jr, *Forest mensuration.* (John Wiley & Sons, Hoboken, New Jersey ed. 4th, 2003), pp. 447.
50. M. G. R. Cannell, Woody biomass of forest stands. *For. Ecol. Manage.* **8**,299-312 (1984).
51. M. Simard, N. Pinto, J. B. Fisher, A. Baccini, Mapping forest canopy height globally with spaceborne lidar. *Journal of Geophysical Research: Biogeosciences* **116** (2011).
52. N. L. Stephenson, P. J. van Mantgem, Forest turnover rates follow global and regional patterns of productivity. *Ecol. Lett.* **8**,524-531 (2005).
53. ESRI, “Release 10.3 of Desktop, ESRI ArcGIS” (Environmental Systems Research Institute, Redlands, CA, 2014)
54. R Core Team, “R: A language and environment for statistical computing” (R Foundation for Statistical Computing, Vienna, Austria, 2013)
55. A. Di Gregorio, L. J. Jansen, “Land Cover Classification System (LCCS): classification concepts and user manual” (FAO, Department of Natural Resources and Environment, Rome, Italy, 2000)
56. P. Legendre, Spatial autocorrelation: trouble or new paradigm? *Ecology* **74**,1659-1673 (1993).
57. J. Liang, Mapping large-scale forest dynamics: a geospatial approach. *Landscape Ecol.* **27**,1091-1108 (2012).
58. J. Pinheiro, D. Bates, S. DebRoy, D. Sarkar, R Development Core Team, *nlme: Linear and Nonlinear Mixed Effects Models.* (2011), vol. R package version 3.1-101.
59. N. A. C. Cressie, *Statistics for spatial data.* (J. Wiley, New York, ed. Rev., 1993), pp. 900.
60. P. Legendre, N. L. Oden, R. R. Sokal, A. Vaudor, J. Kim, Approximate analysis of variance of spatially autocorrelated regional data. *J. Classif.* **7**,53-75 (1990).
61. A. Liaw, M. Wiener, Classification and regression by randomForest. *R News* **2**,18-22 (2002).
62. L. Magee, R<sup>2</sup> measures based on Wald and likelihood ratio joint significance tests. *The American Statistician* **44**,250-253 (1990).
63. M. C. Hansen *et al.*, High-resolution global maps of 21st-century forest cover change. *Science* **342**,850-853 (2013).
64. E. J. Pebesma, Multivariable geostatistics in S: the gstat package. *Computers & Geosciences* **30**,683-691 (2004).

65. E. D. Schulze *et al.*, Opinion Paper: Forest management and biodiversity. *Web Ecology* **14**,3 (2014).
66. R. Waring *et al.*, Why is the productivity of Douglas-fir higher in New Zealand than in its native range in the Pacific Northwest, USA? *For. Ecol. Manage.* **255**,4040-4046 (2008).
67. R. Costanza *et al.*, Changes in the global value of ecosystem services. *Global Environ. Change* **26**,152-158 (2014).
68. BLS, in *BLS Handbook of Methods*. (US Department of Labor, Washington, DC, 2015). We used the online CPI calculator at: <http://data.bls.gov/cgi-bin/cpicalc.pl>.
69. T. Crowther *et al.*, Mapping tree density at a global scale. *Nature* **525**,201-205 (2015).
70. The tree drawings in the diagram were based on actual species from the GFB plots. The scientific names of the species were (clockwise from the top): *Handroanthus albus*, *Liriodendron tulipifera*, *Hamamelis virginiana*, *Araucaria heterophylla*, *Quercus mongolica*, *Ravenala madagascariensis*, *Salix babylonica*, *Adansonia digitata*, *Phoenix dactylifera*, and *Cupressus sempervirens*. Handdrawings were made by RK Watson.
71. Elevation consists mostly of ground-measured data and the missing values were replaced with the highest-resolution topographic data generated from NASA's Shuttle Radar Topography Mission-SRTM.
72. R. J. Hijmans, S. E. Cameron, J. L. Parra, P. G. Jones, A. Jarvis, Very high resolution interpolated climate surfaces for global land areas. *International Journal of Climatology* **25**,1965-1978 (2005).
73. A. Trabucco, R. J. Zomer, in *CGIAR Consortium for Spatial Information*. (2009).
74. N. Batjes, "World soil property estimates for broad-scale modelling (WISE30sec)" (ISRIC-World Soil Information, Wageningen, 2015)
75. D. M. Olson, E. Dinerstein, The Global 200: Priority ecoregions for global conservation. *Annals of the Missouri Botanical Garden*,199-224 (2002).

## ACKNOWLEDGMENTS

We are grateful to all the people and agencies that helped in collection ~~and~~, compilation, and coordination of the field data, including but not limited to T. Malone, J. Crowe, M. Sutton, J. Lovett, P. Munishi, ~~R. Miina~~ M. Rautiainen, staff members from the Seoul National University Forest, and all persons who made the two Spanish Forest Inventories possible especially the main coordinators, R. Villaescusa (IFN2) and J.A. Villanueva (IFN3). This work was supported in part by West Virginia University under the USDA McIntire-Stennis Funds WVA00104 and WVA00105; the University of Minnesota Department of Forest Resources and Institute on the Environment; the Architecture and Environment Department of Italcementi Group, Bergamo (Italy); a Marie Skłodowska Curie fellowship; Polish National Science Center Grant 2011/02/A/NZ9/00108, the French ANR (CEBA: ANR-10-LABX-0025) and the General Directory of State Forest National Holding DB; General Directorate of State Forests, Warsaw, Poland; (Research Projects No. 1/07 and OR/2717/3/11); the 12th Five-Year Science and Technology Support Project (Grant No. 2012BAD22B02) of China; the U.S. Geological Survey and the Bonanza Creek Long Term Ecological Research Program funded by the National Science Foundation and the U.S. Forest Service (any use of trade, firm, or product names is for descriptive purposes only and does not imply endorsement by the U.S. Government); National Research Foundation of Korea (NRF-2015R1C1A1A02037721), Korea Forest Service (S111215L020110, S211315L020120 and S111415L080120) and Promising-Pioneering Researcher Program through Seoul National University (SNU) in 2015; Core funding for Crown Research Institutes from the New Zealand Ministry of Business, Innovation and Employment's Science and Innovation Group; the DFG Priority Program 1374 Biodiversity Exploratories; Chilean research grants FONDECYT No. 1151495 and 11110270; Natural Sciences and Engineering Research Council of Canada (RGPIN-2014-04181); Brazilian Research grants CNPq 312075/2013 and FAPESC 2013/TR441 supporting Santa Catarina State Forest Inventory (IFFSC); General Directorate of State Forests, Warsaw, Poland; Bavarian State Ministry for Nutrition, Agriculture, and Forestry project W07; Bavarian State Forest Enterprise (Bayerische Staatsforsten AöR); German Science Foundation for project PR 292/12-1; European Union for funding the COST Action FP1206 EuMIXFOR; FEDER/COMPETE/POCI under Project POCI-01-0145-FEDER-006958 and FCT - Portuguese Foundation for Science and Technology under the project UID/AGR/04033/2013; Swiss National Science Foundation Grant 310030B\_147092; and the European Union's Horizon 2020 research and innovation programme within the framework of the MultiFUNGtionality Marie Skłodowska-Curie Individual Fellowship (IF-EF) under grant agreement No 655815.

We thank the following agencies and organization for providing the data: the United States Department of Agriculture (USDA) Forest Service; School of Natural Resources and Agricultural Sciences, University of Alaska Fairbanks; the Ministère des Forêts, de la Faune et des Parcs du Québec (Canada); the Alberta Department of Agriculture and Forestry, the Saskatchewan Ministry of the Environment, and Manitoba Conservation and Water Stewardship

(Canada); the [LUCAS programme for the Ministry the Environment \(NZ National Vegetation Survey Databank \(New Zealand\)\)](#); Italian and Friuli Venezia Giulia Forest Services; ~~the Thünen Institute of Forest Ecosystems (Germany (Italy))~~; Bavarian State Forest Enterprise (Bayerische Staatsforsten AöR) ~~and the Thünen Institute of Forest Ecosystems (Germany)~~; Queensland Herbarium (Australia); Forestry Commission of New South Wales (Australia); Instituto de Conservação da Natureza e das Florestas (Portugal). All TEAM data were provided by the Tropical Ecology Assessment and Monitoring (TEAM) Network, a collaboration between Conservation International, the Smithsonian Institute and the Wildlife Conservation Society, and partially funded by these institutions, the Gordon and Betty Moore Foundation, [the Valuing the Arc Project \(Leverhulme Trust\)](#), and other donors; The Exploratory plots of FunDivEUROPE received funding from the European Union Seventh Framework Programme (FP7/2007-2013) under grant agreement no. 265171. The Chinese Comparative Study Plots (CSPs) were established in the framework of BEF-China, funded by the German Research Foundation (DFG FOR891); Data collection in Middle Eastern countries was supported by the Spanish Agency for International Development Cooperation (Agencia Española de Cooperación Internacional para el Desarrollo, AECID) and Fundación Biodiversidad, in cooperation with the governments of Syria and Lebanon.

Finally, we would like to extend our thanks to the editor and two reviewers who provided constructive and helpful comments to help us further improve this paper. The data used in this manuscript are provided in the supplementary materials (Data Table S1-S2).

## **SUPPLEMENTARY MATERIALS**

Figs. S1 to ~~S2~~[S3](#)

Data Tables S1 to S2

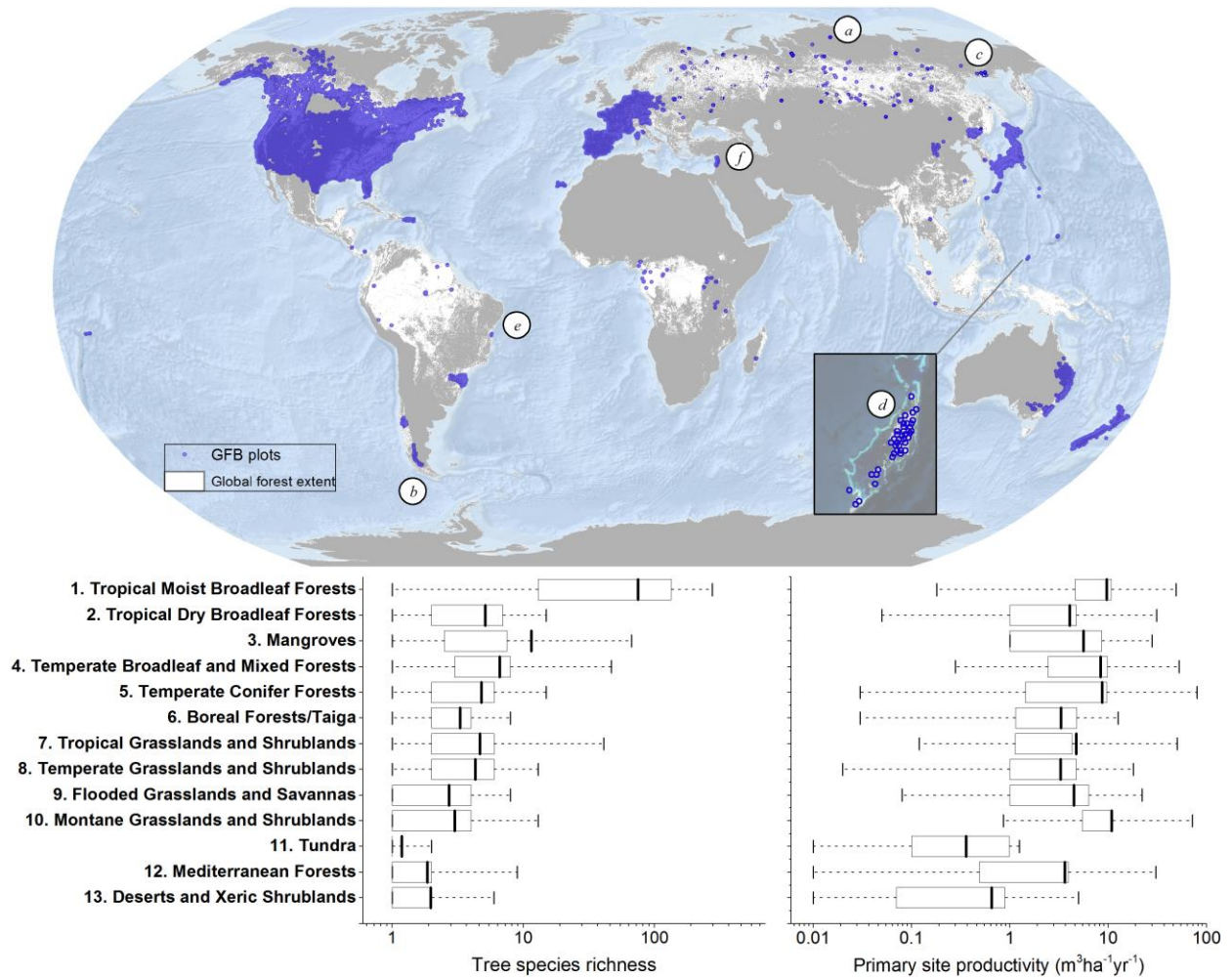


**Fig.1. Global forest biodiversity (GFB) ground-sourced data were collected from *in situ* re-measurement of 777,126 permanent sample plots consisting of over *thirty million* trees across 8,737 species.** GFB plots extend across 13 ecoregions (vertical axis, delineated by the World Wildlife Fund where extensive forests occur within all the ecoregions (69)), and 44 countries and territories. Ecoregions are named for their dominant vegetation types, but all contain some forested areas. GFB plots cover a significant portion of the global forest extent (white), including some of the most unique forest conditions: (a) the northernmost (73°N, Central Siberia, Russia), (b) southernmost (52°S, Patagonia, Argentina), (c) coldest (-17°C annual mean temperature, Oimyakon, Russia), (d) warmest (28°C annual mean temperature, Palau, USA) plots, and (e) most diverse (405 tree species on the 1-ha plot, Bahia, Brazil). Plots in war-torn regions (e.g. f) were assigned fuzzed coordinates to protect the identity of the plots and collaborators. The box plots show the mean and interquartile range of tree species richness and primary site productivity (both on a common logarithmic scale) derived from ground-measured tree- and plot-level records. The complete list of species was presented in Data Table S2.

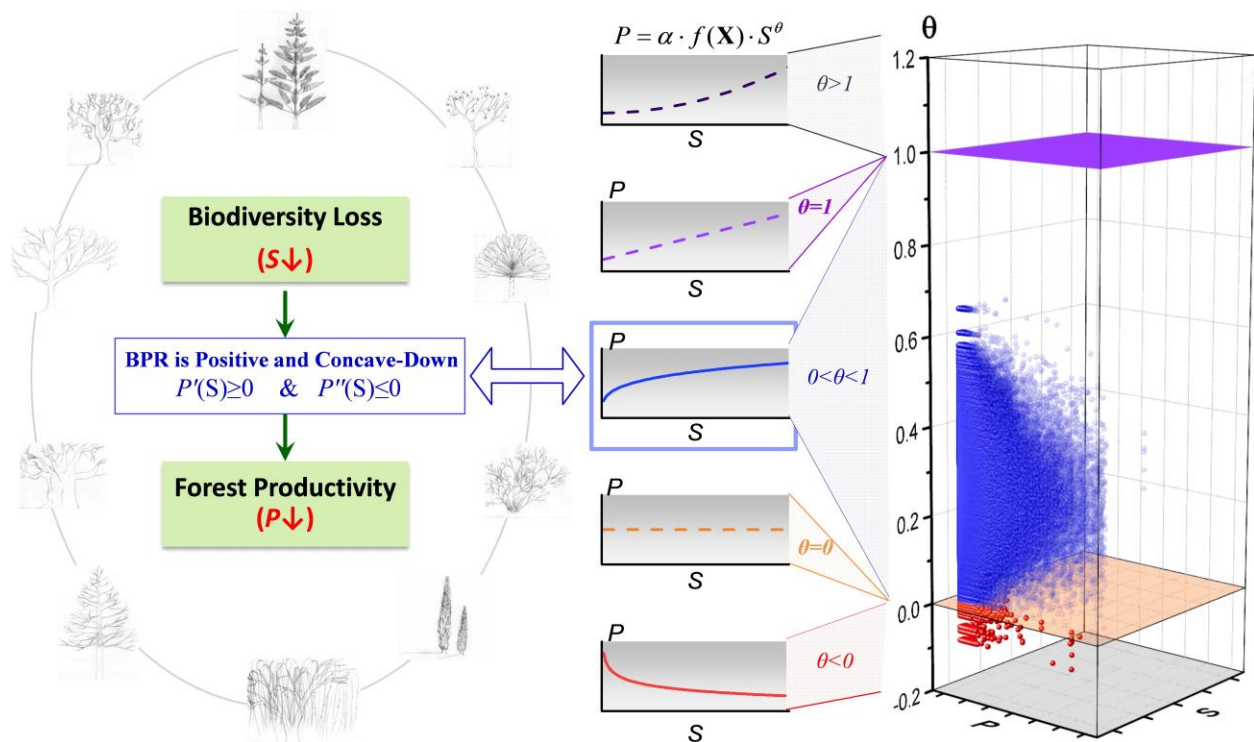


**Fig.2. Theoretical positive and concave-down biodiversity–productivity relationship supported by empirical evidence drawn from the GFB data.** The diagram (left) demonstrates that under the theoretical *positive and concave-down* (i.e. monotonically and degressively increasing) BPR (3, 26, 27), loss in tree species richness may reduce forest productivity (70). **Functional curves in the center** represent different BPR under different values of elasticity of substitution ( $\theta$ ).  $\theta$  values between 0 and 1 correspond to the positive and concave-down BPR (blue curve). **The 3D scatter plot (right)** shows  $\theta$  values we estimated from observed productivity ( $P$ ), species richness ( $S$ ), and other covariates. Out of 5,000,000 estimates of  $\theta$  (mean=0.26, SD=0.09), 4,993,500 fell between 0 and 1 (blue), whereas only 6500 were negative (red), and none was equal to zero, or was greater than or equal to 1. In other words, the positive and concave-down BPR was supported by 99.9% of our estimates.

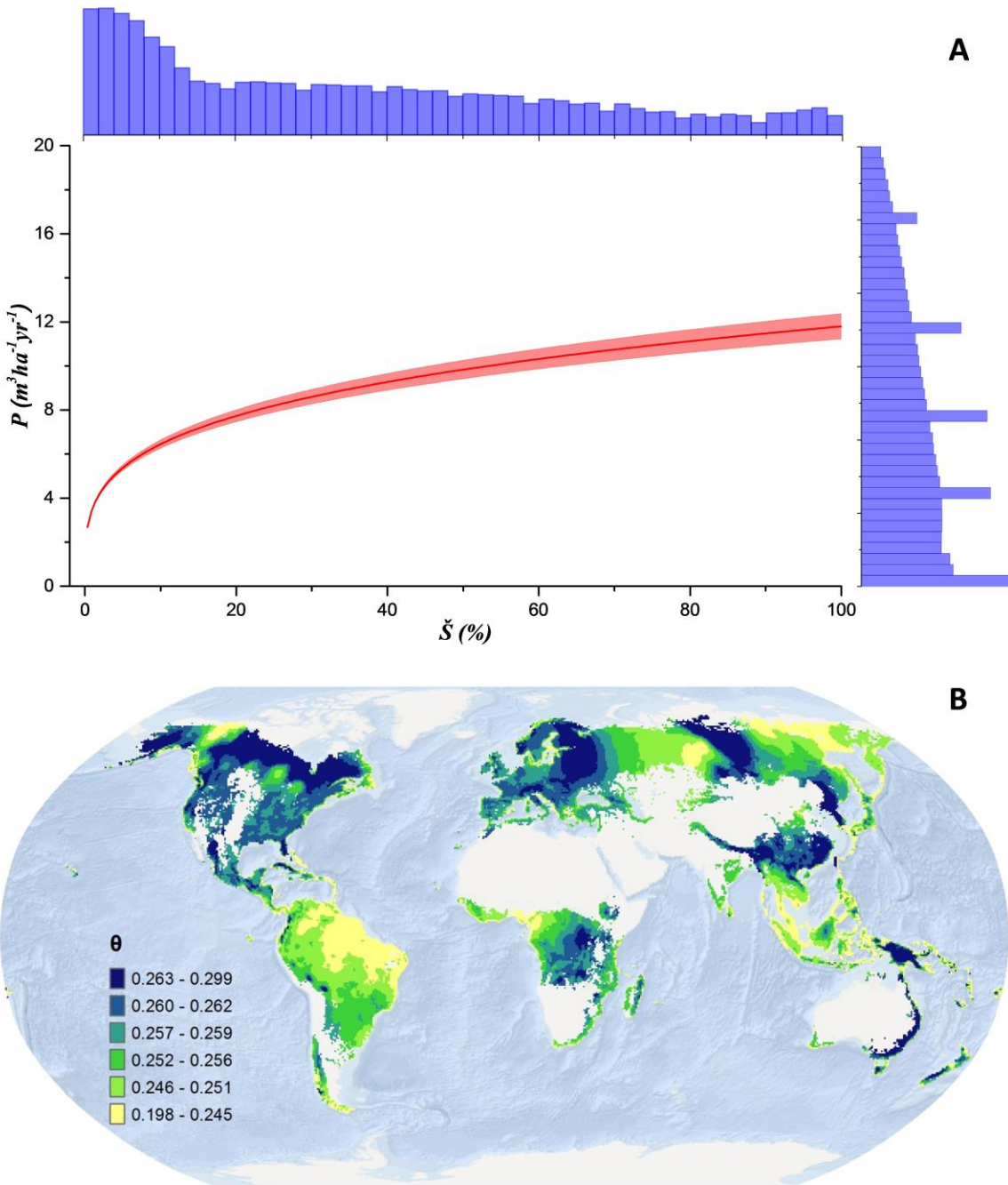


**Fig.3. The estimated global effect of biodiversity on forest productivity was *positive and concave-down* (A) and revealed considerable geospatial variation across forest ecosystems worldwide(B). (A) Global effect of biodiversity on forest productivity (red line with pink bands representing 95 percent confidence interval) corresponds to a global average elasticity of substitution ( $\theta$ ) value of 0.26, with climatic, soil, and other plot covariates being accounted for and kept constant at sample mean. Relative species richness ( $\bar{S}$ ) is in the horizontal axis, and productivity ( $P$ ,  $\text{m}^3\text{ha}^{-1}\text{yr}^{-1}$ ) in the vertical axis (histograms of the two variables on top and right in the logarithm scale). (B)  $\theta$  represents the strength of the effect of tree diversity on forest productivity. Spatially explicit values of  $\theta$  were estimated using universal kriging (see Materials and Methods) across the current global forest extent (effect sizes of the estimates were shown in Fig.5), whereas blank terrestrial areas were non-forested.**

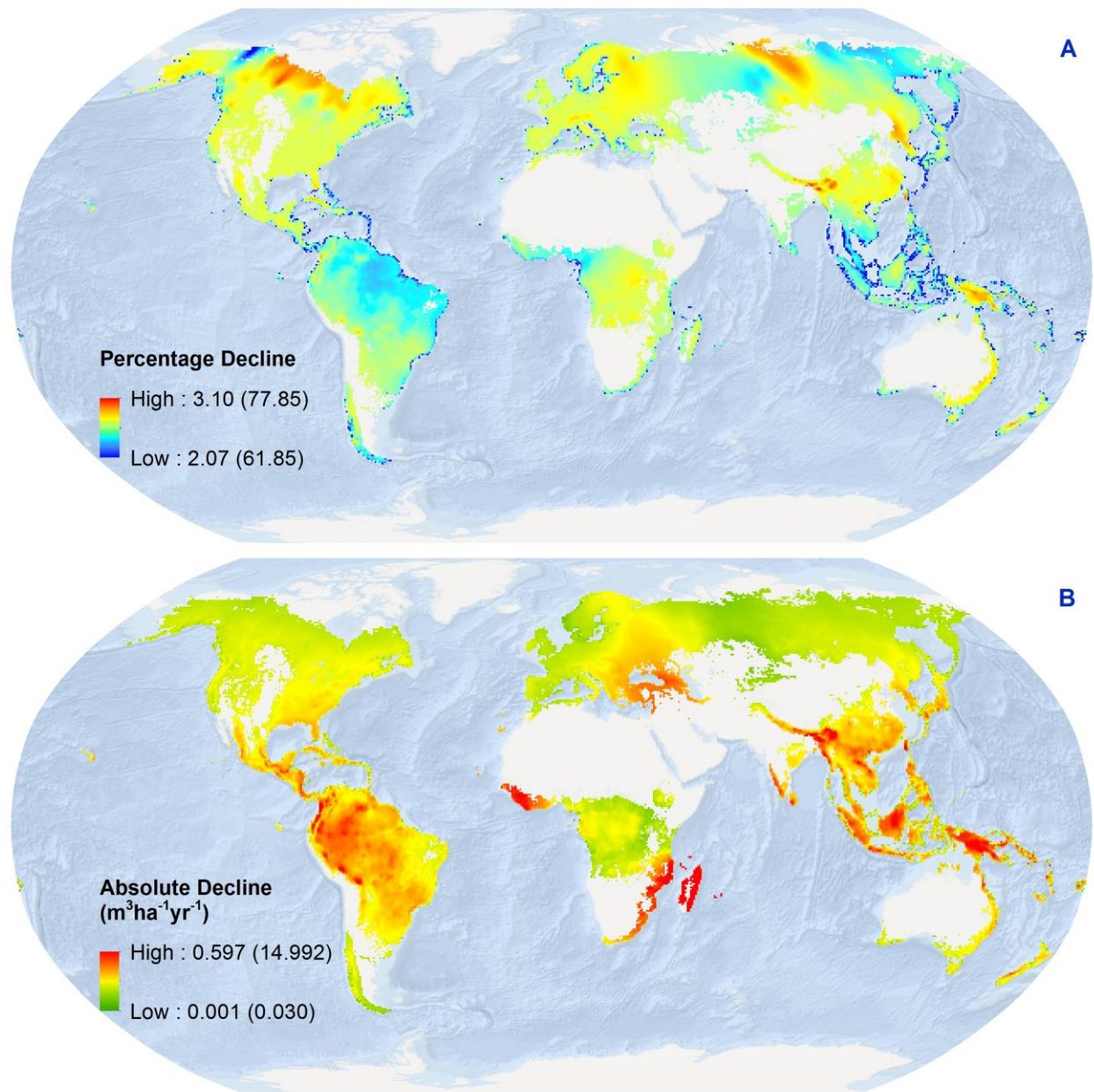


**Fig.4. Estimated percentage(A) and absolute(B) decline in forest productivity under 10 and 99 percent decline in current tree species richness (values in parentheses correspond to 99 percent).** (A) Percent decline in productivity was calculated based on the general BPR model (Eq.1) and estimated worldwide spatially explicit values of the elasticity of substitution (Fig.3B). (B) Absolute decline in productivity, was derived from the estimated elasticity of substitution (Fig.3B) and estimates of global forest productivity (Fig.S1). The first 10 percent reduction in tree species richness would lead to  $0.001\text{--}1.138 \text{ m}^2\text{ha}^{-1}\text{yr}^{-1}$  decline in periodic annual increment, which accounts for 2–3 percent of current forest productivity. The raster data are displayed in 50-km resolution with a three-standard deviation stretch.

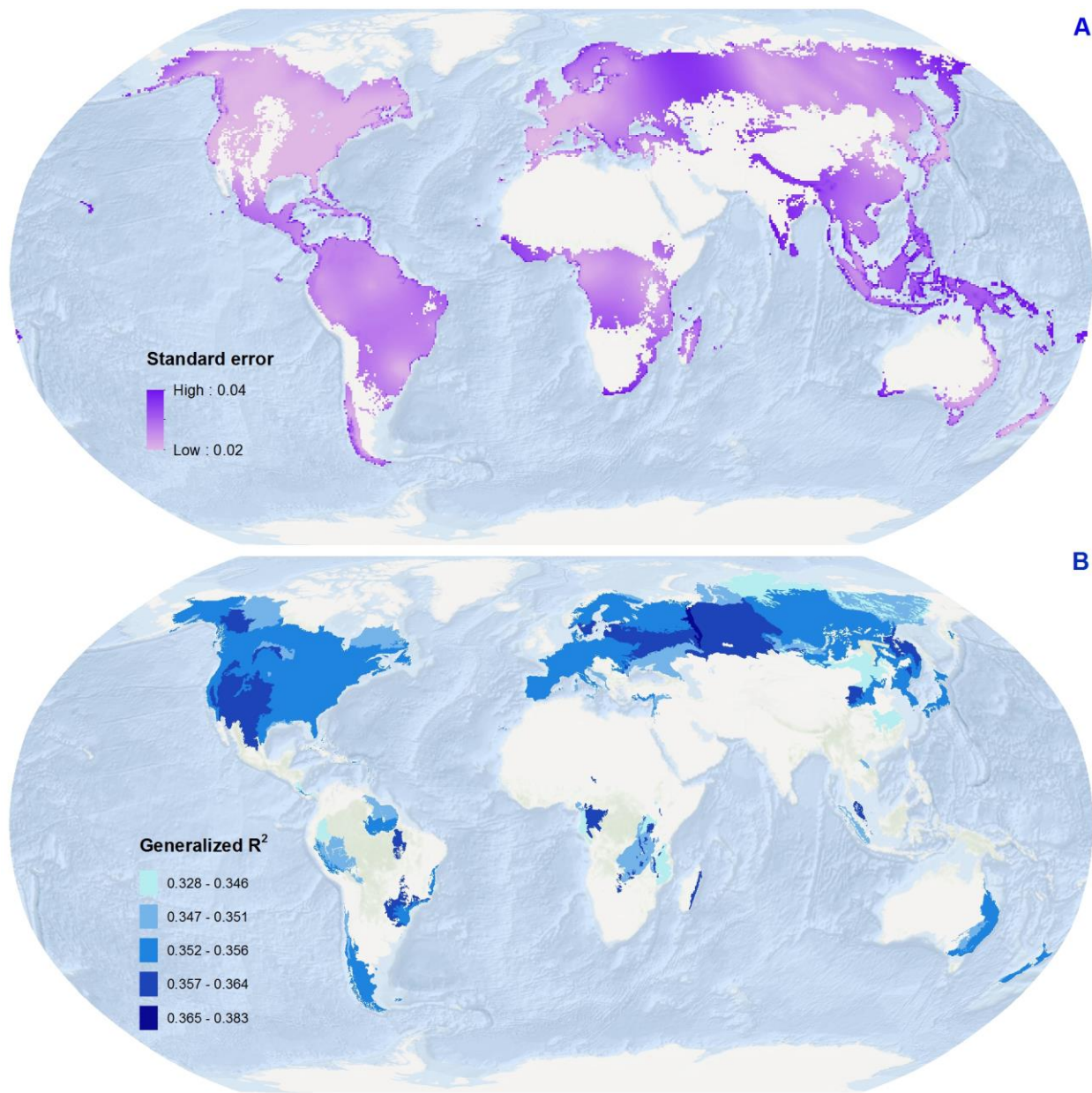


**Fig.5. Standard error (A) and generalized  $R^2$  (B) of the spatially explicit estimates of elasticity of substitution ( $\theta$ ) across the current global forest extent.** Standard error increased as a location was farther from those sampled. The generalized  $R^2$  values were derived with a geostatistical nonlinear mixed-effects model for GFB sample locations, and thus (B) only cover a subset of the current global forest extent.

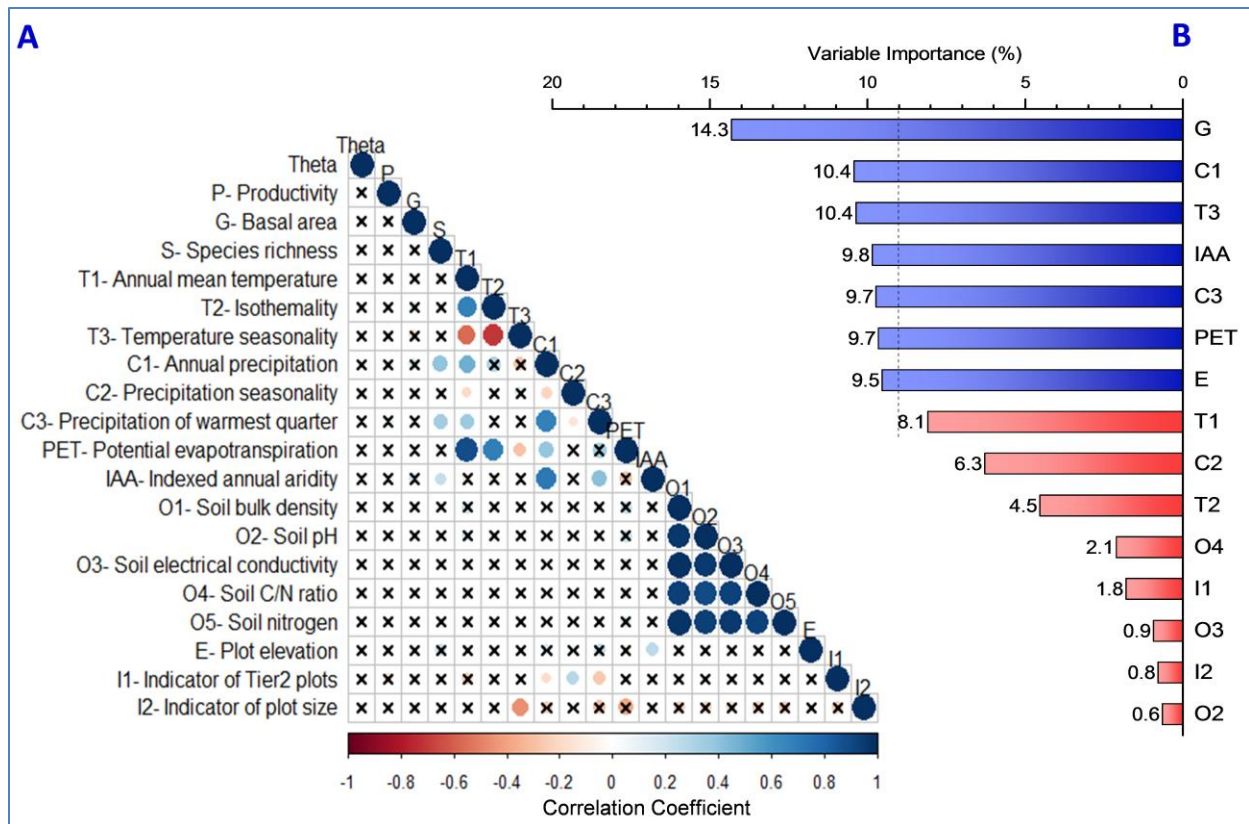


**Fig.6. Correlation matrix (A) and importance values (B) of potential variables for the geospatial random forest analysis.** There were a total of 15 candidate variables from three categories, namely plot attributes, climatic variables, and soil factors (see Table 1 for a detailed description). Correlation coefficients between these variables were represented by sizes and colors of circles, and × marks insignificant-coefficients not significant at  $\alpha=0.05$  level (A). Variable importance (%) values were determined by the geospatial random forest (see Materials and Methods). Variables with importance values exceeding the 9% threshold line (blue) were selected as control variables in the final geospatial random forest models (B). Elasticity of substitution (coefficient), productivity (dependent variable), and species richness (key explanatory variable) were not ranked in the variable importance chart, as they were not potential covariates.

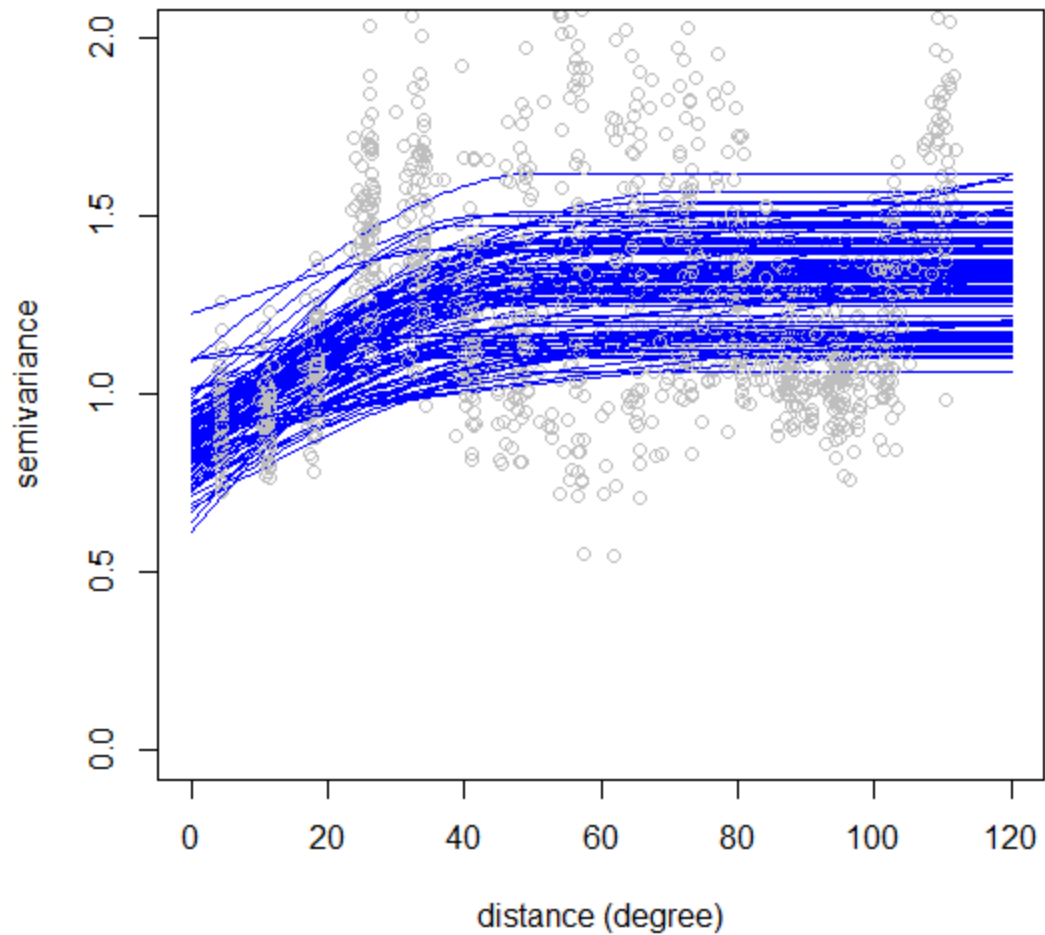


**Fig.7. Semivariance (gray circles) and estimated spherical variogram models (blue curves) obtained from geospatial random forest.** There was a general trend that semivariance increased with distance, *i.e.* spatial dependence of  $\theta$  weakened as the distance between any two GFB plots increased. The final spherical models had nugget=0.8, range=50 degrees, and sill=1.3. To avoid identical distances, all plot coordinates were jittered by adding normally distributed random noises.

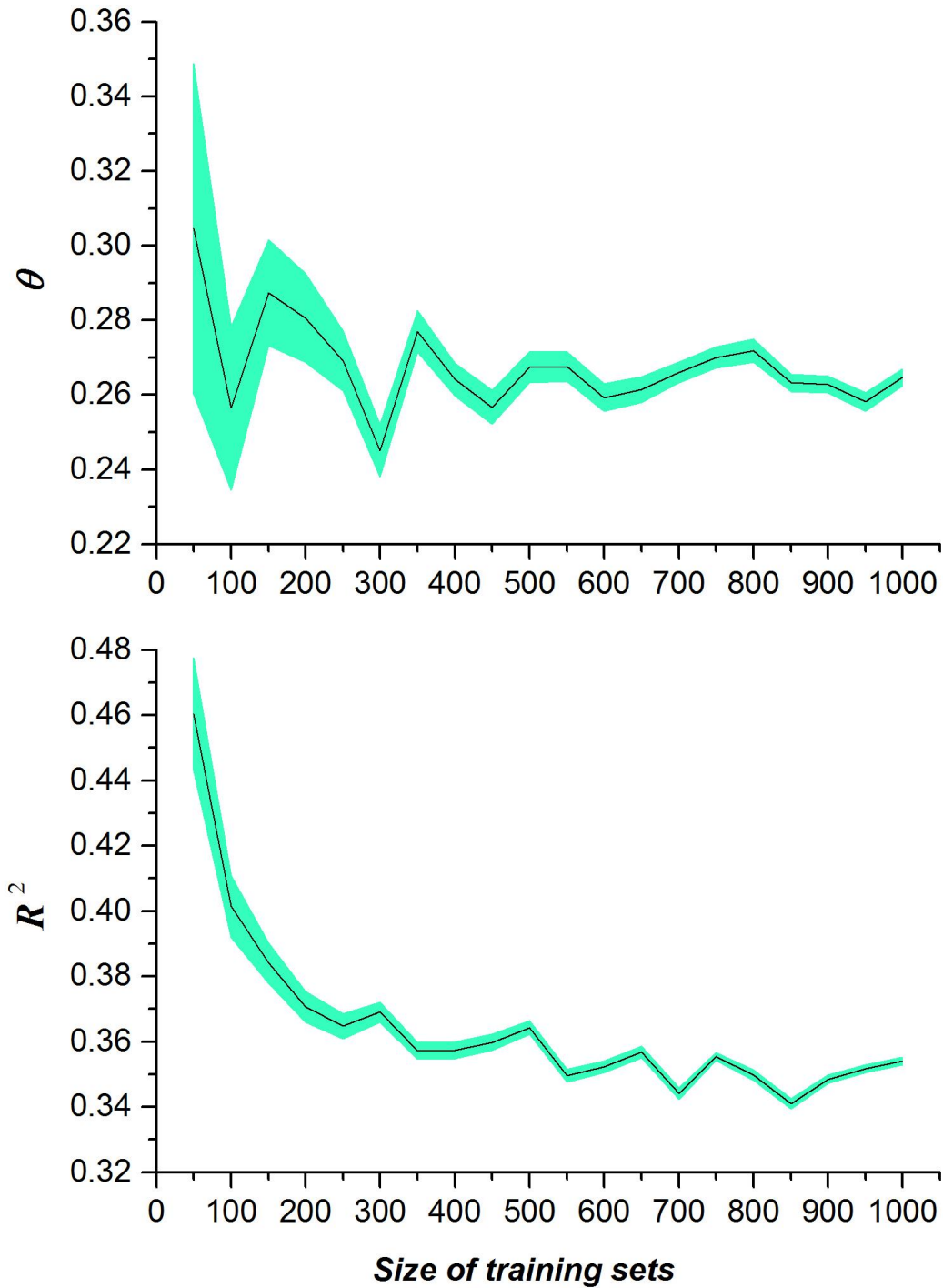


**Fig.8.** Effect of the size of training sets used in the geospatial random forest on estimated elasticity of substitution ( $\theta$ ) and generalized  $R^2$ . Mean (solid line) and standard error band (green area) were estimated with 100 randomly selected (with replacement) training sets for each of the 20 size values (between 50 and 1000 GFB plots, with an increment of 50).

**Table 1. Definition, unit, and summary statistics of key variables.**

Variable	Definition	Unit	Mean	Std.	Source	Nominal Resolution
<b>Response variables</b>						
<i>P</i>	Primary forest productivity measured in periodic annual increment in stem volume (PAI)	$\text{m}^3 \cdot \text{ha}^{-1} \cdot \text{yr}^{-1}$	7.57	14.52	Author generated from ground-measured data	
<b>Plot Attributes</b>						
<i>S</i>	Tree species richness, the number of live tree species observed on the plot	unitless	5.79	8.64	ground-measured	
<i>A</i>	Plot size, area of the sample plot	ha	0.04	0.12	ground-measured	
<i>Y</i>	Elapsed time between two consecutive inventories	year	8.63	11.62	ground-measured	
<i>G</i>	Basal area, total cross-sectional area of live trees measured at 1.3-1.4 m above ground	$\text{m}^2 \cdot \text{ha}^{-1}$	19.00	18.94	Author generated from ground-measured data	
<i>E</i>	Plot elevation	m	469.30	565.92	G/SRTM(71)	
<i>I<sub>1</sub></i>	Indicator of plot tier <i>I<sub>1</sub></i> =1 if a plot was Tier-2, <i>I<sub>1</sub></i> =0 if otherwise	unitless	0.23	0.42	Author generated from ground-measured data	
<i>I<sub>2</sub></i>	Indicator of plot size <i>I<sub>2</sub></i> =1 when $0.01 \leq ps < 0.05$ , <i>I<sub>2</sub></i> =2 when $0.05 \leq ps < 0.15$ , <i>I<sub>2</sub></i> =3 when $0.15 \leq ps < 0.50$ , <i>I<sub>2</sub></i> =4 when $0.50 \leq ps < 1.00$ , where <i>ps</i> was plot size (ha.)	unitless	1.43	0.80	Author generated from ground-measured data	
<b>Climatic Covariates</b>						
<i>T<sub>1</sub></i>	Annual mean temperature	0.1°C	108.4	55.92	WorldClim v.1(72)	1 km <sup>2</sup>
<i>T<sub>2</sub></i>	Isothermality	unitless index*100	35.43	7.05	WorldClim v.1	1 km <sup>2</sup>
<i>T<sub>3</sub></i>	Temperature seasonality	Std.(0.001°C)	7786.00	2092.39	WorldClim v.1	1 km <sup>2</sup>
<i>C<sub>1</sub></i>	Annual precipitation	mm	1020.00	388.35	WorldClim v.1	1 km <sup>2</sup>
<i>C<sub>2</sub></i>	Precipitation seasonality (coefficient of variation)	unitless%	27.54	16.38	WorldClim v.1	1 km <sup>2</sup>
<i>C<sub>3</sub></i>	Precipitation of warmest quarter	mm	282.00	120.88	WorldClim v.1	1 km <sup>2</sup>
<i>PET</i>	Global Potential Evapotranspiration	$\text{mm} \cdot \text{yr}^{-1}$	1063.43	271.80	CGIAR-CSI(73)	1 km <sup>2</sup>
<i>IAA</i>	Indexed Annual Aridity	unitless index*10 <sup>-4</sup>	9915.09	4512.99	CGIAR-CSI	1 km <sup>2</sup>
<b>Soil Covariates</b>						
<i>O<sub>1</sub></i>	Bulk density	$\text{g} \cdot \text{cm}^{-3}$	0.70	0.57	WISE30sec v.1(74)	1 km <sup>2</sup>
<i>O<sub>2</sub></i>	pH measured in water	unitless	3.72	2.80	WISE30sec v.1	1 km <sup>2</sup>
<i>O<sub>3</sub></i>	Electrical conductivity	$\text{dS} \cdot \text{m}^{-1}$	0.44	0.76	WISE30sec v.1	1 km <sup>2</sup>
<i>O<sub>4</sub></i>	C/N ratio	unitless	9.64	7.78	WISE30sec v.1	1 km <sup>2</sup>
<i>O<sub>5</sub></i>	Total nitrogen	$\text{g} \cdot \text{kg}^{-1}$	2.71	4.62	WISE30sec v.1	1 km <sup>2</sup>
<b>Geographic Coordinates and Classification</b>						
<i>x</i>	Longitude in WGS84 datum	degree				
<i>y</i>	Latitude in WGS84 datum	degree				
<i>Ecoregion</i>	Ecoregion defined by World Wildlife Fund(75)					

**Table 2. Parameters of the global geospatial random forest model in 10,000 iterations of 500 randomly selected (with replacement) GFB plots.** Mean and standard error (S.E.) of all the parameters were estimated using bootstrapping. Effect sizes were represented by the Akaike information criterion (AIC), Bayesian information criterion (BIC), and generalized  $R^2$  ( $G-R^2$ ). Const: Constant.

	<i>Loglik</i>	<i>AIC</i>	<i>BIC</i>	$G-R^2$	Coefficients								
					<i>const</i>	$\theta$	<i>G</i>	<i>T3</i>	<i>C1</i>	<i>C3</i>	<i>PET</i>	<i>IAA</i>	<i>E</i>
Mean	<b>-761.41</b>	<b>1546.71</b>	<b>1597.08</b>	<b>0.354</b>	<b>3.816</b>	<b>0.2625243</b>	<b>0.014607</b>	<b>-0.000106</b>	<b>0.001604</b>	<b>0.001739</b>	<b>-0.002566</b>	<b>-0.000134</b>	<b>-0.000809</b>
S.E.	<b>0.54</b>	<b>1.10</b>	<b>1.13</b>	<b>0.001</b>	<b>0.011</b>	<b>0.0009512</b>	<b>0.000039</b>	<b>0.000001</b>	<b>0.000008</b>	<b>0.000008</b>	<b>0.000009</b>	<b>0.000001</b>	<b>0.000002</b>
<b>Iteration</b>													
1	-756.89	1537.78	1588.35	0.259	4.299	0.067965	0.014971	-0.000100	0.002335	0.001528	-0.003019	-0.000185	-0.000639
2	-801.46	1626.91	1677.49	0.281	3.043	0.167478	0.018232	-0.000061	0.000982	0.002491	-0.001916	-0.000103	-0.000904
3	-768.71	1561.41	1611.99	0.357	5.266	0.299411	0.008571	-0.000145	0.002786	0.002798	-0.003775	-0.000258	-0.000728
4	-775.19	1574.37	1624.95	0.354	4.273	0.236135	0.016808	-0.000126	0.001837	0.003755	-0.003075	-0.000182	-0.000768
5	-767.66	1559.32	1609.89	0.248	2.258	0.166024	0.018491	-0.000051	0.000822	0.002707	-0.001575	-0.000078	-0.000553
6	-773.76	1571.52	1622.10	0.342	3.983	0.266962	0.018675	-0.000113	0.001372	0.001855	-0.002824	-0.000101	-0.000953
7	-770.26	1564.53	1615.10	0.421	4.691	0.353071	0.009602	-0.000127	0.002390	-0.001151	-0.003337	-0.000172	-0.000441
...													
2911	-778.21	1580.43	1631.00	0.393	3.476	0.187229	0.020798	-0.000069	0.001826	0.001828	-0.002695	-0.000135	-0.000943
2912	-755.35	1534.71	1585.28	0.370	2.463	0.333485	0.013165	-0.000005	0.001749	0.000303	-0.002447	-0.000119	-0.000223
2913	-800.52	1625.03	1675.61	0.360	4.526	0.302214	0.021163	-0.000105	0.001860	0.001382	-0.003207	-0.000166	-0.000974
2914	-725.89	1475.78	1526.36	0.327	2.639	0.324987	0.013195	-0.000057	0.001322	0.000778	-0.001902	-0.000080	-0.000582
2915	-753.64	1531.28	1581.85	0.324	4.362	0.202992	0.014003	-0.000146	0.001746	0.002229	-0.002844	-0.000143	-0.000750
2916	-796.75	1617.50	1668.08	0.307	3.544	0.244332	0.010373	-0.000118	0.002086	0.002510	-0.002667	-0.000152	-0.000650
2917	-746.88	1517.77	1568.34	0.348	4.427	0.290416	0.008630	-0.000107	0.002203	-0.000314	-0.002770	-0.000155	-0.000945
...													
9997	-775.08	1574.17	1624.74	0.313	1.589	0.193865	0.012525	-0.000056	-0.000589	0.000550	-0.000066	-0.000155	-0.000839
9998	-781.20	1586.40	1636.98	0.438	5.453	0.412750	0.014459	-0.000169	0.002346	0.002175	-0.003973	-0.000117	-0.000705
9999	-734.72	1493.43	1544.01	0.387	4.238	0.211103	0.013415	-0.000118	0.001896	0.002450	-0.002927	-0.000076	-0.000648
10000	-776.14	1576.28	1626.86	0.355	2.622	0.468073	0.015632	-0.000150	-0.000093	0.001151	-0.000756	-0.000019	-0.000842